CoCO2
Prototype system for a Copernicus CO_2 service

D2.2 Prior Emission data 2021 documentation

CoCO2

Prototype system for a Copernicus CO_2 service

D2.2 Prior data 2021 documentation report

Dissemination Level: Public/ Confidential

Author(s): Hugo Denier van der Gon (TNO)

Date: 01/01/2023

Version: 1.2

Contractual Delivery Date: 31/08/2022

Work Package/ Task: WP2/ T2.1

Document Owner: TNO

Contributors: BSC, CNRS Lab AERO, DLR, JRC, LSCE, Mercator-ocean, MPG-Jena, TNO

Status: v1-2 revised after internal review

CoCO2: Prototype system for a Copernicus CO_2 service

Coordination and Support Action (CSA)

H2020-IBA-SPACE-CHE2-2019 Copernicus evolution – Research activities in support of a European operational monitoring support capacity for fossil CO2 emissions

Project Coordinator: Dr Richard Engelen (ECMWF)

Project Start Date: 01/01/2021

Project Duration: 36 months

Published by the CoCO2 Consortium

Contact:
ECMWF, Shinfield Park, Reading, RG2 9AX, richard.engelen@ecmwf.int

The CoCO2 project has received funding from the European Union's Horizon 2020 research and innovation programme under grant agreement No 958927.

Table of Contents

1 Introduction and Summary 6
1.1 Background 6
1.2 Scope of this deliverable 6
1.2.1 Objectives of this deliverable 6
1.2.2 Work performed in this deliverable 6
1.2.3 Deviations and counter measures 6
1.3 Summary and outlook 7
1.3.1 Outlook 8
2 Regional anthropogenic prior emission datasets of ffCO2 and bioCO2 and co-emitted species for 2021 9
2.1 Improvements in the regional TNO GHGco_v5 inventory for year 2021 12
2.2 Extrapolation to recent years 14
2.3 Data availability 17
2.3.1 Contact persons: 17
3 Global anthropogenic prior emission datasets of ffCO2 and bioCO2 and co-emitted species for 2021 18
3.1 Methodology to obtain the 2021 dataset 18
3.2 Emissions data 19
3.2.1 Methane data 19
3.2.2 Trends in CO2ff emission datasets 20
3.3 Data availability 21
3.3.1 Contact persons: 21
4 Global biofuel production and consumption maps 22
4.1.1 Contact persons: 23
5 Regional biogenic prior emission datasets for 2018 and 2021 (2017-2021) 24
5.1 Model 24
5.2 Spatial coverage and resolution 24
5.3 Regional blocks 24
5.4 Temporal resolution 25
5.5 Data Access 25
5.5.1 Contact person: 25
6 Global biogenic prior emission datasets for 2021 26
6.1 Details of data processing: 26
6.2 Results for Net Ecosystem Exchange 27
6.3 Details and access of global biogenic flux data 28
6.3.1 Contact persons: 28
7 Global ocean flux datasets for 2021 29
7.1 Data availability 31

7.1.1 Contact persons: 32
8 LULUCF datasets for 2018-2020 33
8.1 Documentation 33
8.2 Data access 33
8.2.1 Contact person: 33
9 Emission height profiles by source sector 34
9.1 Regional emission height profiles 34
9.1.1 contact persons 34
9.2 Global emission height profiles 35
9.2.1 contact person: 35
10 References 36

1 Introduction and Summary

This deliverable report describes the characteristics of the regional and global prior (anthropogenic and biogenic) emissions datasets compiled for the year 2021 in CoCO2 WP2 Task 2.1. It gives a brief overview of the methodology and the resulting products, and provides information on data access and contact persons for each product.

1.1 Background

The aim of Task 2.1 is to provide state-of-the-art emission data as input for WP3 (Development of global modelling and data assimilation capacity in an MVS), WP4 (Local and regional modelling and data assimilation) and the CO2MVS in general. Data assimilation efforts in WP3 and WP4 require prior information on emissions that is spatially explicit and complete. This implies that both anthropogenic and biogenic fluxes are included, both for the regional (European) domain (WP4) and the global domain (WP3). An important limitation of the current emission inventories is that they are based on data that partly become available with a lag of at least 2 years. Therefore, one of the focus points of Task 2.1 is to develop new methodologies and use additional data sources to be able to deliver reliable prior emission data with a shorter lag time. While the first prior emission data covered 2018 to best accommodate and fit with the models and satellite data used in WP3 and WP4, the current prior emission dataset covers the year 2021 and relies on new methods to deal with the fact that some of the official emission data is not yet available.

1.2 Scope of this deliverable

1.2.1 Objectives of this deliverable

The objective is to compile a regional and global emission dataset for 2021 consisting of individual components that modellers can use and that covers all relevant species and sectors, including anthropogenic, biosphere and ocean fluxes. The aim is to base the dataset on a consistent bottom-up approach at regional or global scale to ensure consistency and transparency.

1.2.2 Work performed in this deliverable

The work for this deliverable has resulted in seven emission products:

- A dataset of regional anthropogenic emissions (chapter 2)
- A dataset of global anthropogenic emissions (chapter 3)
- A dataset of global biofuel consumption and production fluxes (chapter 4)
- A dataset of regional biosphere fluxes (chapter 5)
- A dataset of global biosphere fluxes (chapter 6)
- A dataset of (global) ocean fluxed (chapter 7)

Next to this an introduction to a global land use, land use change, and forestry (LULUCF) dataset for 2021 is provided (chapter 8). Default emission height profiles by sector for point sources for the regional and global scale are provided in chapter 9.

1.2.3 Deviations and counter measures

The planned delivery date was August 31st 2022. The final delivery of the datasets was delayed until the end of 2022, because of various delays in either data processing, later input data availability or first trials that revealed inconsistencies which needed to be solved before providing the data to users. Especially for the latter several meetings between task 2.1 and WP3 were organised between September- November 2022 to have an interactive discussion on choices to be made taking both data quality and timeliness into account.

1.3 Summary and outlook

This deliverable report documents the development of a Prior Emission Dataset (PED) for the year 2021. The PED consists of different components that are complementary such as anthropogenic emissions, biogenic land-based fluxes, and ocean fluxes for a) the global scale and b) the regional European scale. The report also provides a brief description and access to two datasets that provide complementary information on lateral carbon fluxes and LULUCF carbon fluxes. In a separate chapter brief information on emission height for the anthropogenic regional and the global data set is provided by source sector.

Each product is described in an individual chapter which provides contact persons for further details and access to the data. As such this document is a guide to the other CoCO2 WPs on what data has been prepared and how to get access to it.

Making a 2021 PED in year 2022, so within less than a year delay, was substantially more challenging than preparing the previous deliverable D1.1 2018 PED. This is mostly because for the year 2018 more auxiliary data are already published, calibrated, validated and/or available in easy accessible formats. For each of the core products described in this report large improvements and/or novel methods were used. To give an impression several of those are listed here:

- The global biogenic emission dataset (chapter 6) uses a completely new methodology based on a machine learning model trained on flux tower data (~ 13 million hourly NEE observations from 250 flux towers) and using satellite observations from MODIS and meteorological data. This allowed for an enormous jump in temporal and spatial resolution (from 0.5 to 0.05 degree hourly). Not only year 2021 was produced but the time series 2018-2021 is made available so a consistent set for the COCO2 2018 and 2021 is produced. A remarkable result of the new product is that the big and unrealistic sink in the tropics present in the previous product (FLUXCOM1) is no longer present in the new product which is a clear improvement.
- The regional biogenic fluxes at ~1x1 km hourly for the European domain (chapter 5) are extended back to 2017 and extra years 2019 and 2020 were added to have a complete timeseries 2017-2021 as requested, but originally not foreseen, by WP4. Already with the 2018 PED there were complications with the data size but now a storage solution was found through German DKRZ computing centre for 8.7 TB in total.
- For the global ocean fluxes (chapter 7) an entirely new methodology was proposed and developed with first test sets being produced since September 2022. The ocean pCO2 observation-based (obs) product from CMEMS-LSCE (this is the current input for the CAMS-CO2 system) is assimilated into the MOi's ocean reanalysis system which results in the provision of "hybrid obs/model" air-sea CO2 fluxes with a strong increase in spatial and temporal resolution (respectively: 0.25° x 0.25°, daily).
- The regional anthropogenic emissions (Chapter 2), unlike the PED 2018, cannot make use of reported emissions data to EMEP or UNFCCC since these will only become available mid-2023. Therefore the methodology used to compile the current regional emission inventory for the year 2021 builds on tested extrapolation techniques developed in the VERIFY and CAMS emission project. Next to this several important improvements have been implemented especially concerning point source emissions. Here an extra challenge is that the EEA has changed the reporting for industrial facilities (E-PRTR) but the completeness of this new data has considerable limitations and not all countries have contributed or may decide to no longer deliver data (e.g. UK). Moreover, the start of 2021 was still sincerely affected by the COVID-19 pandemic and activity data-based adjustments were made in the emissions especially for the transport sectors, most notably aviation and road transport.
- The global anthropogenic emissions (Chapter 3) also faced substantial challenges because many of the data sets used did not yet provide data for 2021 and simple extrapolation techniques based on historic trends become unreliable due to the disruption by the COVID-19 pandemic. Since the developer of the global GCP dataset CICERO is

also a CoCO2 WP2 partner we were able to discuss possibilities for using the GCP 2021 fossil fuel CO2 emissions to scale the more detailed sector based PED2018 dataset. This has resulted in the current CoCO2 PED 2021 dataset.

1.3.1 Outlook

Providing prior emission data for two years (2018 and 2021) for both anthropogenic and natural systems with high temporal and spatial resolution for both the European regional and global at two scales is a major effort and one of the most important deliverables of CoCO2 WP2. We are confident that the data described in this report will contribute to the overall success of the CoCO2 project and the CO2MVS development.

In Year 3 of CoCO2 a discussion can be had on whether it is necessary to have all the prepared data stored in a central place and where this should be. This is not trivial as the data size of especially the high resolution, hourly biospheric flux data is enormous and cannot be simply hosted on a project sharepoint or equivalent. Although storage of all products in a central place sounds attractive and logical it may not be the most functional solution. Therefore more discussion on this is needed including why do we do this exactly, and who can facilitate this within reasonable effort and budget requirements.

2 Regional anthropogenic prior emission datasets of ffCO2 and bioCO2 and co-emitted species for 2021

The regional European emission dataset for 2021 has been compiled and delivered in October 2022. This work is done in collaboration with and building on CAMS_81 and the CHE and VERIFY projects, but introduces several important improvements. A main feature of the 2021 regional emission dataset is that the inventory is compiled for the previous calendar year (current year -1) while the official emission reporting is only available up to the current year -2. To do this, emissions have been extrapolated from the officially reported emissions for 2019, to year 2021, using a method combining economic and physical indicators, and also accounting for the COVID-19 effect where appropriate.

Table 1: Characteristics of the anthropogenic emissions for greenhouse gases and selected co-emitted species for the European domain for 2021

Description	**TNO GHGco v5 regional European emissions for 2021**
Product family	Anthropogenic emissions
Species	CO_2_ff[1], CO_2_bf, CO_ff, CO_bf, NO_x, CH_4, NMVOCs
Geographical area	Europe (-30.0°, 60.0°, 30.0°, 72.0°)
Vertical coordinate	Surface with emission height profile by sector
Vertical coverage	Surface flux, area sources and point sources at exact location
Horizontal resolution	0.1° x 0.05° longitude-latitude
Time coverage	2021
Time resolution	Default temporal profiles by GNFR sector with monthly, daily and hourly fractions Country-specific hourly fractions for GNFR sectors F1 – F4, F21, F41 and H
Dissemination mechanism	FTP, Data Server
Data format	NetCDF, CSV
Dissemination time	October 2022

1) ff = fossil fuel, bf = biofuel (solid, liquid or gaseous)

The sector classification of the regional emission data is shown in Table 2. The sector coding follows the GNFR system which is an aggregated version of the NFR (Nomenclature For Reporting) used for Gridding the data (GNFR). This system is used for the emission reporting to EMEP and EU by individual countries, and for consistency reasons has also been implemented in the TNO GHGco v5.0 emission inventory. More details on the sector classification can be found on the CEIP website[1].

To accommodate the use of more specific time profiles for the different road transport subsectors, a version is also provided where GNFR sectors F2 and F4 are disaggregated to distinguish between light duty vehicles and heavy duty vehicles.

[1] http://www.ceip.at/ms/ceip_home1/ceip_home/reporting_instructions/

Table 2: Source sectors following the GNFR Sector nomenclature and short category name

GNFR_Category	GNFR_Category_Name
A	A_PublicPower
B	B_Industry
C	C_OtherStationaryComb
D	D_Fugitives
E	E_Solvents
F	F_RoadTransport
G	G_Shipping
H	H_Aviation
I	I_OffRoad
J	J_Waste
K	K_AgriLivestock
L	L_AgriOther
F1	F_RoadTransport_exhaust_gasoline
F2	F_RoadTransport_exhaust_diesel
F3	F_RoadTransport_exhaust_LPG_gas
F4	F_RoadTransport_non-exhaust
F21	F_RoadTransport_exhaust_diesel_PC_LDV_MOT_MOP
F22	F_RoadTransport_exhaust_diesel_HDV_BUS
F41	F_RoadTransport_non-exhaust_PC_LDV_MOT_MOP
F42	F_RoadTransport_non-exhaust__HDV_BUS

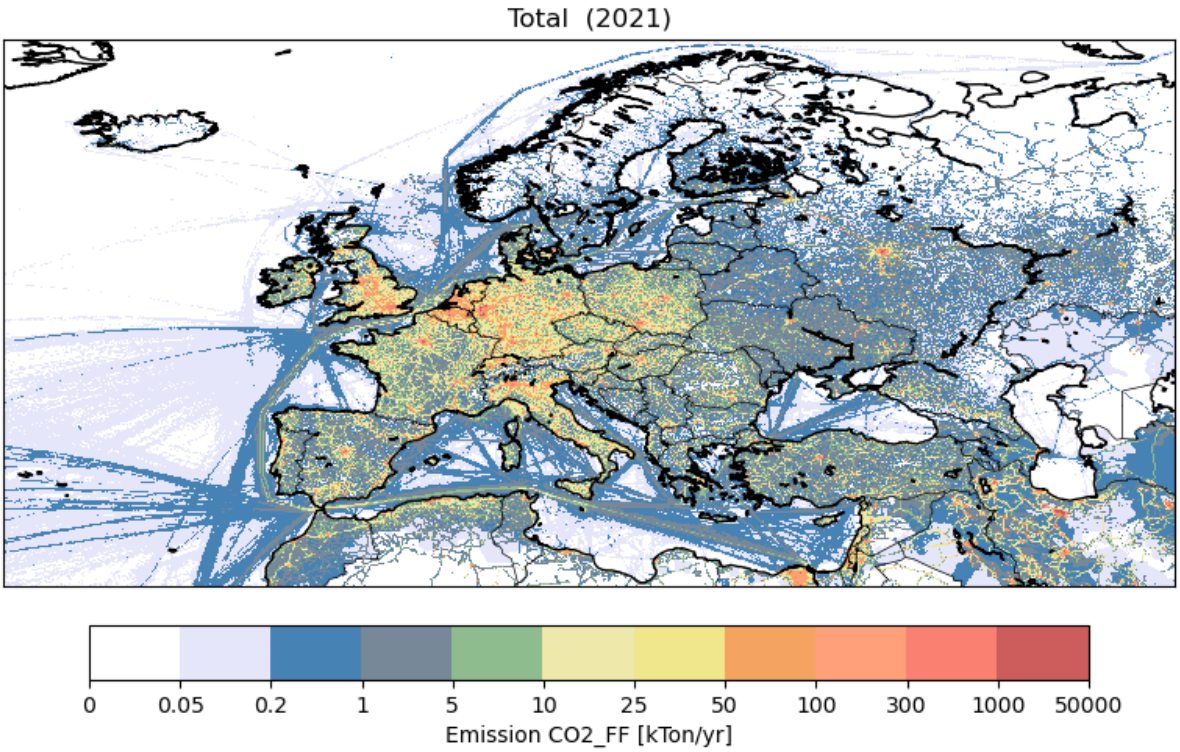

Figure 1: Example of the CO_2 emissions from fossil fuel combustion for 2021 from the TNO_GHGco v5.0 dataset.

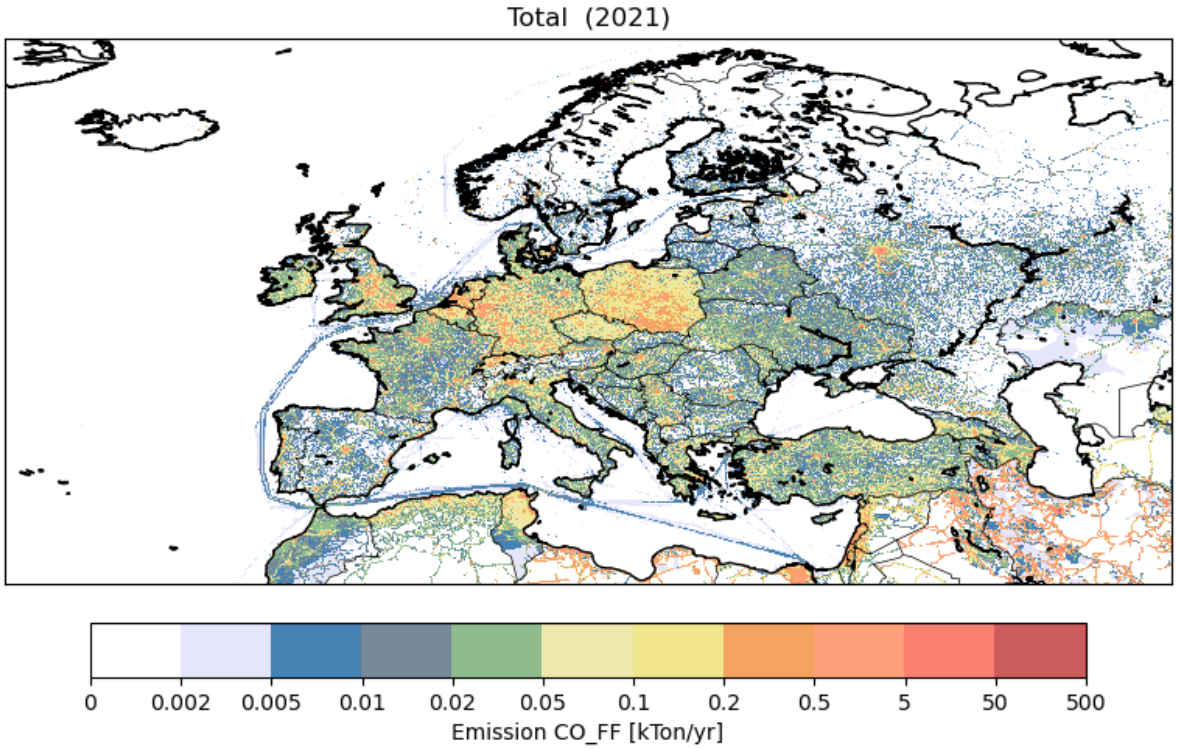

Figure 2: Example of the CO emissions from fossil fuel combustion for 2021 from the TNO_GHGco v5.0 dataset.

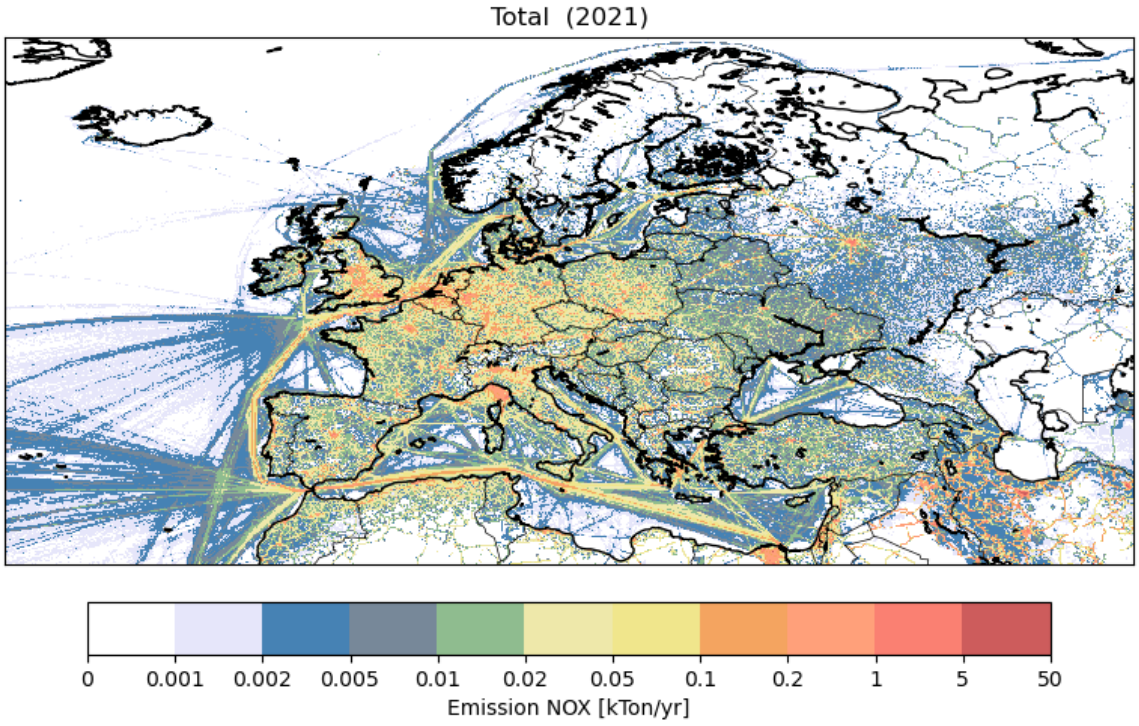

Figure 3: Example of the NOx emissions for 2021 from the TNO_GHGco v5.0 dataset.

2.1 Improvements in the regional TNO GHGco_v5 inventory for year 2021

The methodology used to compile the current regional emission inventory for the year 2021 builds on the methodology used for the previous version for the year 2018, and also builds on extrapolation techniques developed in the CAMS_81 project. Several important improvements have been implemented in this TNO GHGco v5 inventory compared to the previous versions:

- Base emission data for all sectors have been updated to the 2022 reporting to UNFCCC (greenhouse gases) and CLRTAP (air pollutants) for the year 2019. The corrected time series up to 2019 is the basis for the extrapolation or extension to 2021.
- Improvements in spatial proxies, such as the population density map which has been updated to the year 2020 using the latest LandScan Global product, impact multiple sectors and pollutants [2].
- The emissions and spatial allocation of sea shipping emissions are now based on the latest and improved STEAM model by FMI (v. 4.1, Jalkanen and Majamäki, 2021), which, among other improvements, has updated emission factors for various ship types and pollutants. A new addition in the shipping emission model are the methane emissions from engine slip for LNG ships (see Figure 4). Sea shipping emissions have been calculated for 2021, so these are not extrapolated but based on actual AIS (automatic identification signal) monitoring of ship movements. For inland shipping, national reported emission values are used and only the spatial distribution has been based on the STEAM model.

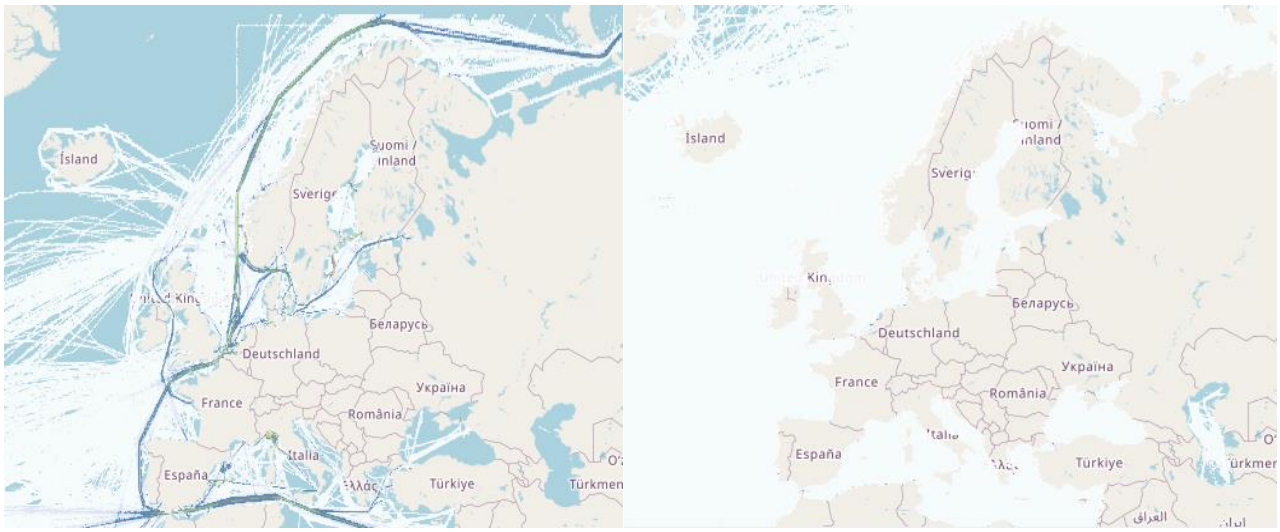

Figure 4: Illustration of methane emissions from sea shipping (GNFR G) in the regional inventory for 2021 (left) and the previous inventory for 2018 (right). In the previous inventory, methane was modelled as a fixed fraction on all NMVOC emissions from shipping. In the new version, methane emissions are specifically modelled for some types of ships (such as LNG ships), but not others, leading to a more realistic pattern of methane emissions

- For power plants and other large industrial point sources, the latest Industrial Emission Dataset containing EPRTR and LCP reporting of industrial facilities, has been linked to the previous data series, providing reported emission data up to 2020 for most facilities. Unfortunately, some countries have not yet provided complete reporting of emissions for individual industrial facilities. For these countries, the facilities share in 2017 emissions is used for the later years.

[2] Rose, A., McKee, J., Sims, K., Bright, E., Reith, A., & Urban, M. (2021). LandScan Global 2020 [Data set]. Oak Ridge National Laboratory. https://doi.org/10.48690/1523378

- An error has been corrected in the allocation of iron/steel production emissions for non-EU countries, which caused a number of missing facilities. This error is associated only with iron/steel as it is related to the specific technology used in iron/steel manufacturing of individual plants. (see Figure 5).

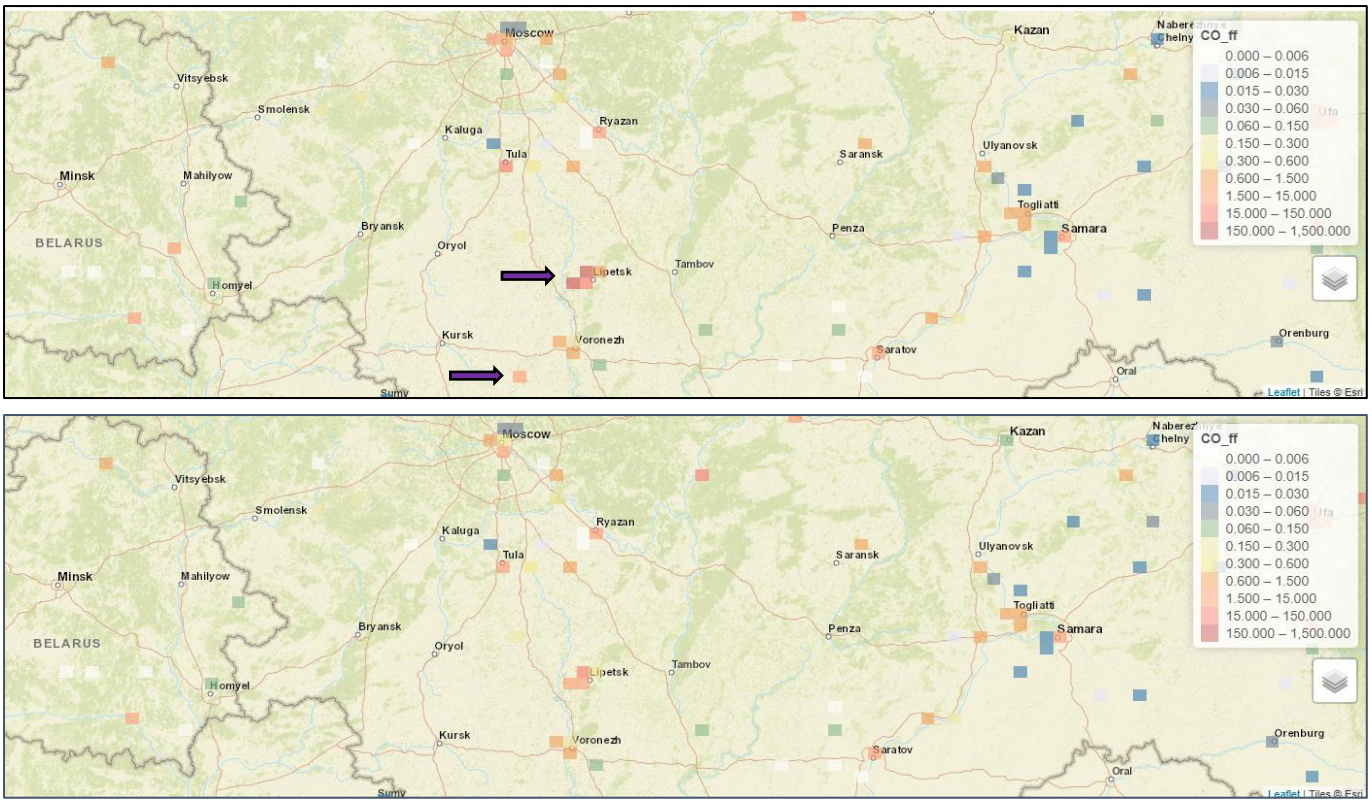

Figure 5: Illustration of CO_ff emissions from industry (GNFR B) in the regional inventory for 2021 (top) and the previous inventory for 2018 (bottom), zoomed into south-west Russia. Following an error correction, several point sources are now included or have their emission values corrected. Purple arrows indicate two examples of changed emissions.

2.2 Extrapolation to recent years

To get emission estimates for the year 2021 in absence of reported emissions, an extrapolation method is applied, following the approach depicted in Figure 6. Simply extrapolating the emissions time series will take into account dominant trends, e.g. the reduction in NO_x emission factors from road transport, but will ignore interannual variability in economic activities or the weather. Therefore, the activity and emission factors are treated separately and combined at the end of the process to estimate emissions.

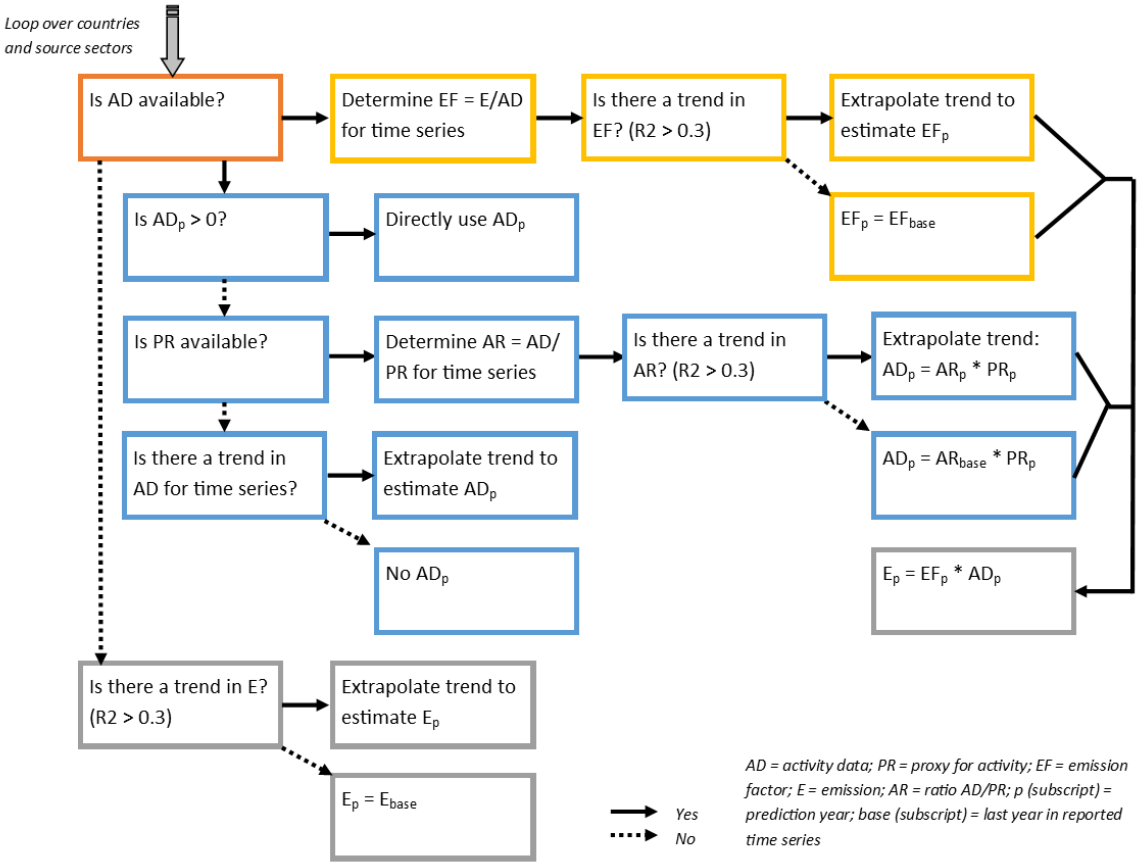

Figure 6: Decision tree for emission calculations for prediction year. Acronyms and meaning of the arrows are explained in the legend at the bottom.

There are two ways to describe the activity:

- Using activity data that can be directly linked to the source sector, such as energy statistics or animal numbers. This is the preferred and most reliable approach.
- Using a generic proxy not directly linked to the source sector to estimate the activity, such as gross domestic product (GDP).

Even if good activity data exist for a specific source sector, sometimes these data are not available for all countries, or the time series do not extend to the year we want to predict. In that case the second option is used by defining a relationship between the activity proxies. An overview of all the data used is given in Table 3. Note that some sub-sectors are defined specifically to support the comparison with the COVID-19 emission reduction factors from the CAMS_COP079 project, even though the same proxy data are used. Most results are shown per aggregated GNFR sector, as this is what is finally delivered as dataset.

Table 3. Overview of activity and proxy data used for each source sector.

Source Sector	Activity data	Period	Proxy data	Period
Public power	Electricity generation (non-renewable)[1]	2008-2021	GDP	Up to 2021
Industry: Refineries	Refinery througput[1]	2008-2021	GDP	Up to 2021
Industry: Chemicals, food/drink	Industrial production index (manufacturing)[2]	2010-2021	GDP	Up to 2021
Industry: Other	Industrial production index (manufacturing)[2]	2010-2021	GDP	Up to 2021
Small combustion	Yearly degree day sum[3]	2005-2021		
Fugitives: Coal mining	Coal production[1]	2008-2021	GDP	Up to 2021
Fugitives: Refineries	Refinery througput[1]	2008-2021	GDP	Up to 2021
Fugitives: Distribution oil products	Industrial production index (manufacturing)[2]	2010-2021	GDP	Up to 2021
Fugitives: Other	Industrial production index (manufacturing)[2]	2010-2021	GDP	Up to 2021
Road transport: Exhaust	Energy consumption in transport sector[4]	2008-2020	GDP	Up to 2021
Road transport: Non-exhaust	Energy consumption in transport sector[4]	2008-2020	GDP	Up to 2021
Inland shipping	CO_2 emissions from inland shipping[5]	2014-2020	GDP	Up to 2021
Agriculture-livestock	Animal numbers (cattle, swine, sheep, other)[6]	2010-2020		
Agriculture-other: Application of manure and fertilizer	Total nutrient N from agricultural fertilizer use[7]	2010-2020	Utilised agr. Area[8]	2007-2020
Agriculture-other: Other	Utilised agriculture area[8]	2007-2020		

[1] Source: BP statistics; [2] Source: Eurostat; [3] Source: ERA5 hourly data, converted to yearly degree day sum using the approach described by Mues et al. (2004); [4] Source: Eurostat; [5] Source: FMI in CAMS_81; [6] Source: FAO; [7] Source: FAO; [8] Source: Eurostat

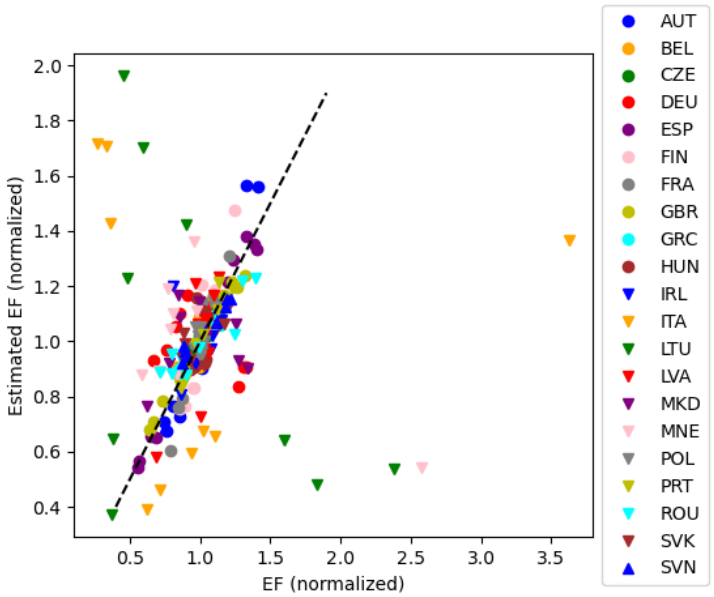

Figure 7. Scatter plot of actual (x-axis) and estimate (y-axis) CO2 emission factor for the public power sector per country for the whole time series. Values are normalized.

For the emission factors (EFs) we look at the full period covered by the activity data to see whether a trend exists in the emissions/activity that we can use to calculate the EF for recent years (again only if $R^2 > 0.3$). Otherwise, the EF of the base year is used.

An exception is the EF of CO_2_ff from the public power sector (GNFR_A). Here, we take into account changes in the fuel mix per country based on power generation data from ENTSO-E

(https://transparency.entsoe.eu/), which are available for different fuel types. An EF adjustment per country is calculated by combining the fuel share to the total power generation and default IPCC emission factors per fuel type. The adjustment factor is specified relative to the base year. This method introduces some uncertainty and can show large deviations from the actual EF, but improves the interannual variability for most countries (Figure 7).

For 2020 a strong impact of the COVID pandemic on country-level emissions was visible. In 2021 there is still a clear impact on road transport and aviation. Therefore, we treat these two sectors separately by 1) calculating a business-as-usual (BAU) and then 2) applying COVID adjustment factors. The BAU scenario follows the same methodology as described before, but now the activity data for 2021 is ignored for the two sectors. The COVID adjustment factors for road transport are based on the work by Guevara et al. (2022), extended to 2021. The adjustment factors for the aviation sector are based on CarbonMonitor (Liu et al, 2020). Since COVID also had an impact on the timing of the emissions, the temporal profiles for road transport and aviation are also based on these adjustment factors and available per country. For all other sectors the regular temporal profiles can be applied.

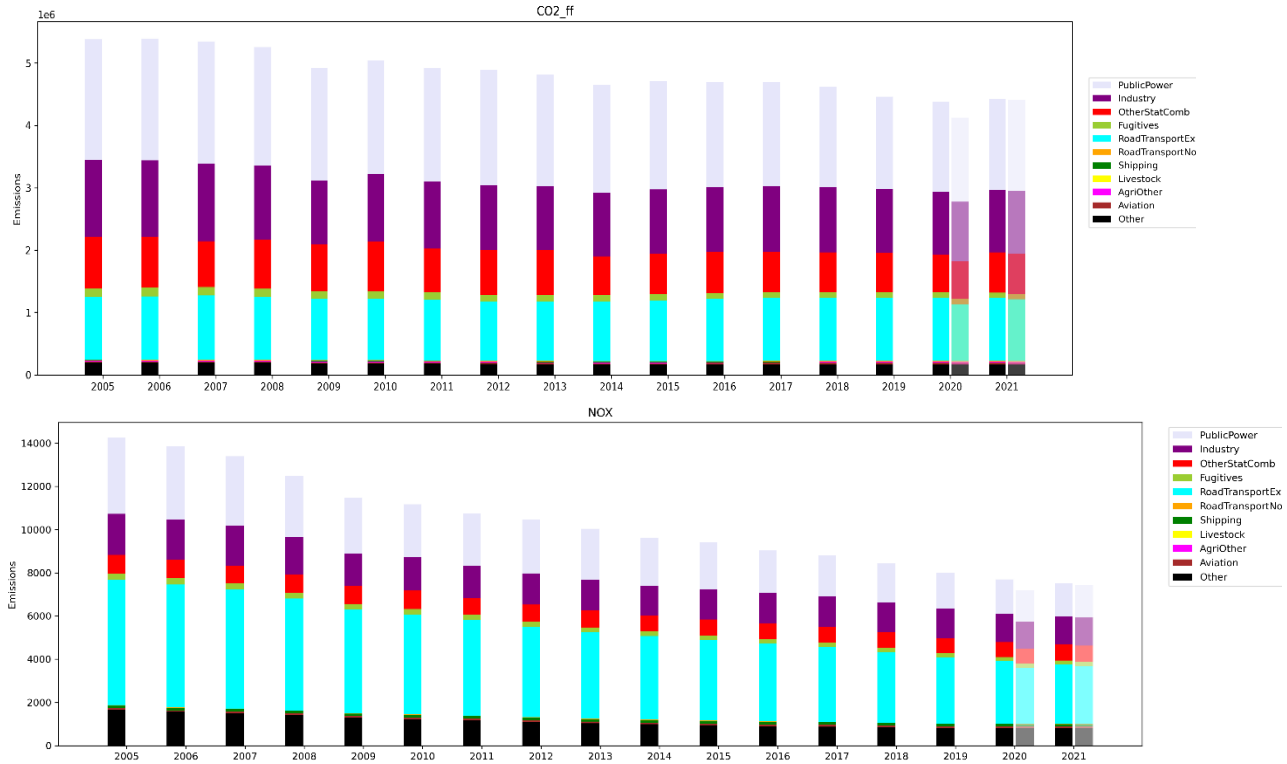

Figure 8. Time series of reported and predicted emissions of CO_2_ff and NOx. Up to 2019 emissions are reported values, for 2020 and 2021 a BAU (dark bars) and COVID (lighter bars) estimate is given.

Resulting time series for CO_2_ff and NO_x are presented in Figure 8. For NO_x a clear impact of COVID is visible for the road transport sector in 2020 and less so in 2021. Figure 9 shows CO_2_ff emission scaling factors for the public power sector for 2021 relative to 2019 (i.e. a scaling factor of 1.1 indicates a 10% increase in 2021 emissions compared to 2019).

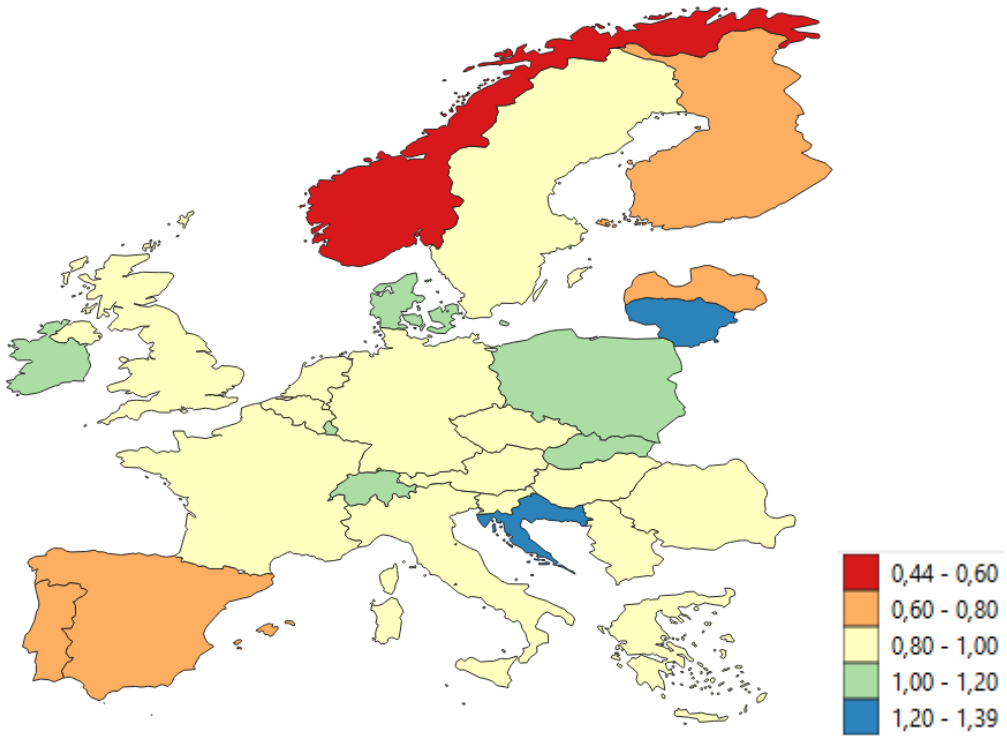

Figure 9: CO_2_ff emission scaling factor for the public power sector. Values indicate the relative difference in emissions for 2021 compared to 2019.

2.3 Data availability

The annual gridded emissions (CoCO2_v5.0_2021) are provided in csv and NetCDF format at a spatial resolution of 0.05°x0.1° (lat-lon). The data are avaible from the TNO ftp site. Username and pass word to access the site have been provided to the users within CoCO2 and can be obtained from one of the contact persons given below. Moreover, temporal profiles to breakdown the annual data to hourly emissions as well as an emission height profile for point sources can be provided with the data upon request.

In the course of 2023 we intend to make the data also available through the Emissions of atmospheric Compounds and Compilation of Ancillary Data (ECCAD) system with a login account (https://eccad3.sedoo.fr/data).

2.3.1 Contact persons:

- hugo.deniervandergon@tno.nl
- jeroen.kuenen@tno.nl
- stijn.dellaert@tno.nl
- ingrid.super@tno.nl

3 Global anthropogenic prior emission datasets of ffCO2 and bioCO2 and co-emitted species for 2021

CoCO2-PED2021 global anthropogenic emissions have been developed for CO_{2ff} and CO_{2bf} for the year 2021 and work is ongoing for CH_4. It was based on Global Carbon Budget 2021 CO_{2ff} emissions and CoCO2-PED2018 inventory that is also developed for CO_{2ff}, CO_{2bf}, CH_4, BC, OC, CO, NOx, SO_2 and NMVOC for the period 2010-2018.

CAMS-GLOB-ANTv5.3 was merged with the DACCIWAv2 inventory to which the temporal profiles from CAMS-GLOB-TEMPO were applied for the period 2010-2018. We used the DACCIWAv2 dataset, which provides African emissions grid maps. DACCIWA-2 is an extension of the regional DACCIWA inventory (Keita et al., 2021; https://doi.org/10.5194/essd-2020-32). The CAMS-GLOB-ANTv5.3 emissions for Africa were then replaced by the DACCIWAv2 emissions to obtain CoCO2-PED2018.

Table 4 shows the correspondence between the different datasets used. The first column shows the sectors in the CAMS-GLOB-ANT dataset and the second the CoCO2-PEDs sectors. The right column provides the species for which emissions by sector are available.

Table 4: Overview of inventories (CAMS-GLOB-ANTv5.3, DACCIWAv2 and CoCO2-PEDs) sectors and species

CAMS-GLOB-ANTv5 sectors	DACCIWAv2 and CoCO2-PED	Species
Power Generation (ENE)	ENERGY_S	CO2ff, CH4, CO, BC, OC, NOx, NMVOCs, SO2
	OTHER	CO2bf, CH4, CO, BC, OC, NOx, NMVOCs, SO2
Indistrial processes (IND)	MANUFACTURING	CO2ff, CO2bf, CH4, CO, BC, OC, NOx, NMVOCs, SO2
Road Transportation (TRO)	TRANSPORTATION	CO2ff, CH4, CO, BC, OC, NOx, NMVOCs, SO2
Non-Road Transportation (TNR)	TRANSPORTATION	CO2ff, CH4, CO, BC, OC, NOx, NMVOCs, SO2
Ships (SHP)	TRANSPORTATION	CO2ff, CH4, CO, BC, OC, NOx, NMVOCs, SO2
Residential (RCO)	SETTLEMENTS	CO2ff, CO2bf, CH4, CO, BC, OC, NOx, NMVOCs, SO2
Fugitive emissions (FEF)	OTHER	CO2ff, CH4, CO, BC, OC, NOx, NMVOCs, SO2
Solvents (SLV)	OTHER	NMVOCs, CH4
Agriculture Livestock (AGL)	OTHER	CH4, NOx, NMVOCs
Agriculture soils (AGS)	OTHER	CH4, NOx, NMVOCs
Solid waste and wastewater (SWD)	ENERGY_A	CO2ff, CO2bf, CH4, CO, BC, OC, NOx, NMVOCs, SO2
Agriculture waste burning (AWB)	OTHER	CO2bf, CH4, CO, BC, OC, NOx, NMVOCs, SO2

3.1 Methodology to obtain the 2021 dataset

The CoCO2-PED2021 dataset is obtained by scaling CoCO2-PED2018 dataset with the annual total values given by the Global Carbon Budget (GCB) for each country (Pers. Comm. Robbie Andrew). Emissions for CoCO2-PED2021 for CO_{2ff} and CO_{2bf} have been developed using the following methodology:

- Gridding of annual total CO_{2ff} data given by GCB for each country
- Disaggregation of these country total values in the same 0.1x0.1 degree grid as CO_{2ff} from CoCO2-PED2018 per sectors in order to obtain the country totals CO_{2ff} provided by GCB.
- Calculation of the ratio of the 2018 CO2 emissions CO_{2bf} /CO_{2ff} for each country from CoCO2-PED2018 data.

- Application of this ratio to the 2021 CO_{2ff} data given by GCB for each country to obtain 2021 CO_{2bf} for each country that has been gridded
- Disaggregation of the country total CO_{2bf} value in the same 0.1x0.1 degree grid as CO_{2bf} from CoCO2-PED2018 per sectors in order to obtain the country totals CO_{2bf}.

3.2 Emissions data

Emissions for CO_{2ff}, CO_{2bf}, CH_4, BC, OC, CO, NOx, SO_2 and NMVOC compounds are available in CoCO2-PED2018 dataset for the period 2010-2018 on monthly basis at a 0.1x0.1 degree in latitude and longitude spatial resolution. However, the COCO2-PED2021 inventory provides CO_{2ff} and CO_{2bf} dataset for the year 2021 on a monthly basis at the same horizontal resolution. For example, Figure 10 shows the emissions of CO_{2ff} for January (top) and July (down) 2021, respectively.

3.2.1 Methane data

CH4 emissions in 2021 are only provided for a limited number of regional and global inventories, we are currently performing comparisons to analyze available 2018-2021 CH4 global emissions to define the most accurate trends for providing a 2021 CH4 emission field.

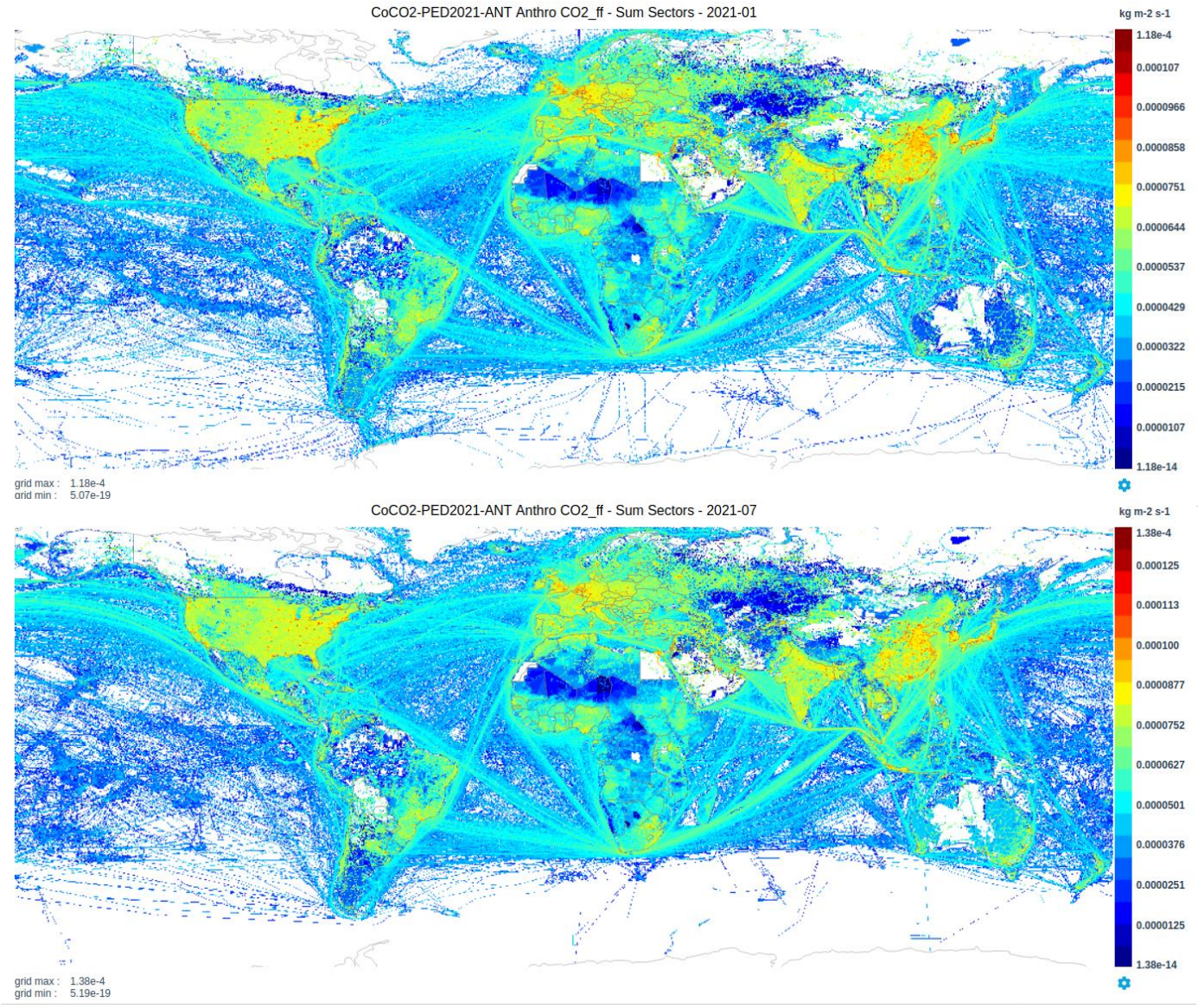

Figure 10 Monthly emissions of CO_{2ff} for January (top) and July (down) 2021 from CoCO2-PED2021 global inventory.

3.2.2 Trends in CO2ff emission datasets

Figure 11 shows the trend in CO2ff emissions over the period 1970-2021 for different global inventories (GCB, Edgarv6.0 & v7.0, CAMS-GLOB-ANTv5.3, COCO2-PED2018 and COCO2-PED2021). CO2ff emissions are rather similar and the largest differences are of the order of 3.5%. CO2ff emissions of CoCO2-PED2018 and CAMS-GLOB-ANTv5.3 are globally the same with CoCO2-PED2018 slightly higher than CAMS-GLOB-ANTv5.3 by 0.25% over the period 2010-2018. GCP is also slightly higher than COCO2-PED2018 (0.57%) during 2010-2012 and is lower than it (0.35%) during 2013-2016. CO2ff emissions for year 2021 from CoCO2-PED2021 (37074 Tg) is between GCP and over global inventories and is slightly higher than GCP (1.61%). It is not possible to say which dataset is better because the datasets are like apples and oranges: For example GCP, unlike EDGAR, is fuel-based and has no detailed sector splits and no-co emitted species. The estimates, however, are close and Figure 11 shows that the CoCO2-PED2021 is giving an estimate comparable to three established inventories but has more detail in terms of source sectors and/or co-emitted species (NOx and CO).

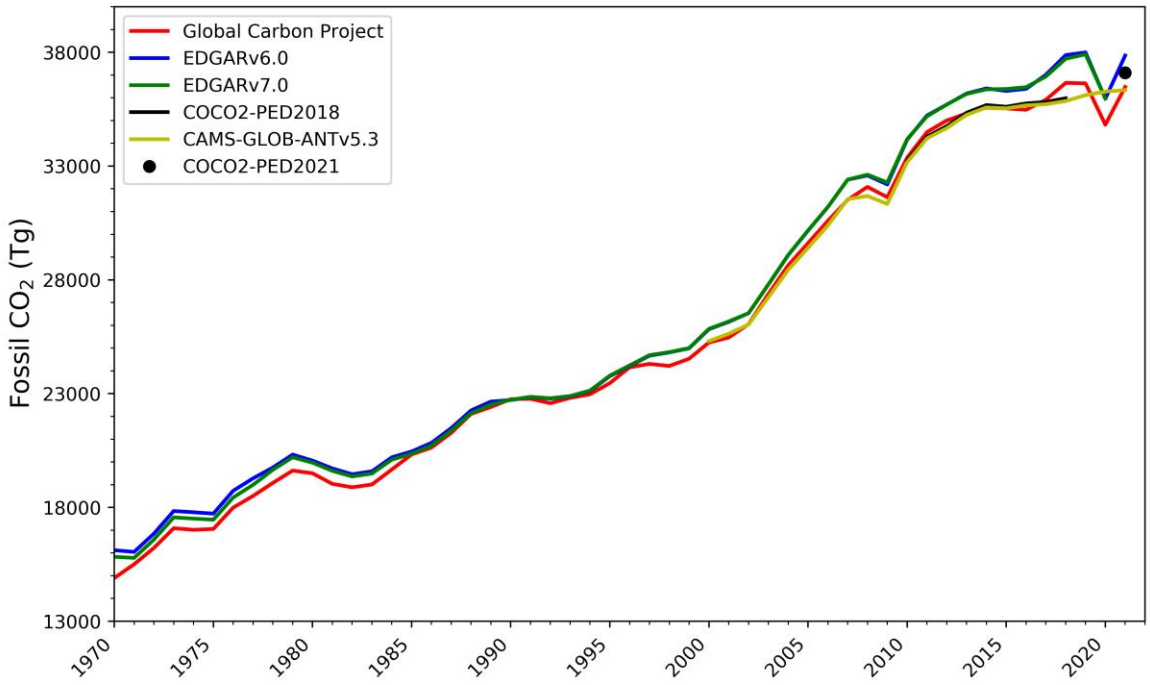

Figure 11: Trend of CO2ff emissions over the period 1970-2021 for different global inventories (GCB, Edgarv6.0 & v7.0, CAMS-GLOB-ANTv5.3, COCO2-PED2018 and COCO2-PED2021 (black dot)).

3.3 Data availability

The monthly gridded emissions (CoCO2-PEDs) are provided in the NetCDF format at a spatial resolution of 0.1°× 0.1° and are available through the Emissions of atmospheric Compounds and Compilation of Ancillary Data (ECCAD) system with a login account (https://eccad3.sedoo.fr/data).

3.3.1 Contact persons:

Claire.granier@aero.obs-mip.fr,

sekou.keita@aero.obs-mip.fr,

antonin.soulie@aero.obs-mip.fr

4 Global biofuel production and consumption maps

The biofuel production and consumption provide an alternative view on CO_2 sources and sinks related to biofuel. It is not to be used directly with the anthropogenic emission and biogenic data sets described in this deliverable report as there will be double counting involved. It is a complementary source of information that will help to inform on the important role of biomass and biofuel in carbon accounting.

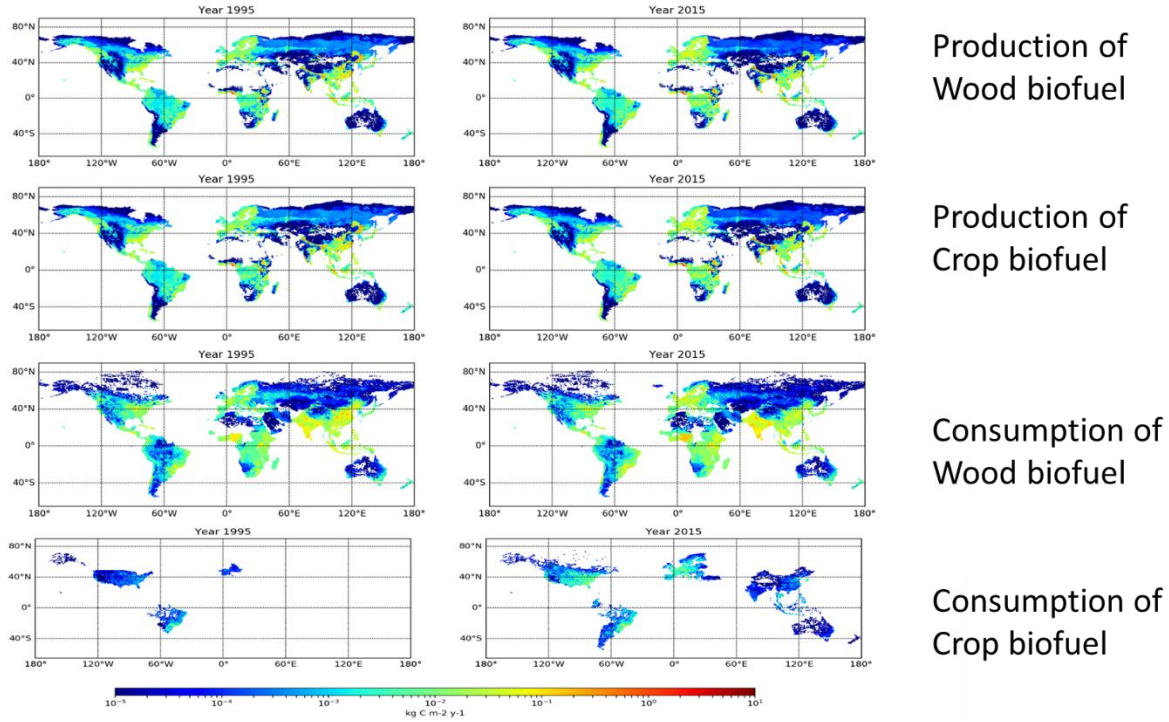

Figure 12 Preliminary maps of wood biofuel and crop biofuel production and consumption in 1995 and 2015 (source LSCE).

For trade fluxes, statistics from the Food and Agriculture Organization of the United Nations (FAO) have been analysed with appropriate conversion factors and disaggregated on the 0.08-degree global grid with a series of proxies and activity maps. River fluxes come from a data-driven climatology. Biofuel sinks and sources from crop and wood have been explicitly included, in collaboration with Yilong Wang (Institute of Geographical Sciences and Natural Resources Research, China). To that end, trade statistics from the International Energy Agency (IEA) and spatial distribution maps from Peking University (PKU) have been included in the processing.

The products are 0.08-deg annual maps with the following variables, in gC m^{-2} yr^{-1}:

- Surface upward mass flux of carbon from crop use including biofuels
- Surface downward mass flux of carbon from crop growth including biofuels
- Surface upward mass flux of carbon from wood use including biofuels
- Surface downward mass flux of carbon from wood production including biofuels
- Surface upward mass flux of carbon from biofuel crop burning
- Surface downward mass flux of carbon from biofuel crop growth
- Surface upward mass flux of carbon from biofuel wood burning
- Surface downward mass flux of carbon from biofuel wood production
- Terrestrial biospheric carbon that is reactive in the inland water network (counted positive)
- Surface upward mass flux of carbon from rivers, lakes and reservoirs

Terrestrial biospheric carbon that is reactive in the inland water network is important in the lateral transfer of organic carbon along the terrestrial-aquatic continuum and an important link in the global carbon (C) cycle. This process should not be ignored when assessing or modelling changes in terrestrial and aquatic C budgets. Much of the input into the inland waters will be of anthropogenic origin but not all. This is a typical example of where separation between anthropogenic and biogenic cannot be easily made.

For further descriptions we refer to Ciais et al. (2022); Deng et al. (2022) and Ciais et al (2007). LSCE will update the data into a v3 in spring 2022 when input data for year 2021 is available.

The latest data can be accessed from:

https://vesg.ipsl.upmc.fr/thredds/fileServer/work/p24cheva/LateralFluxes/lateralfluxes_${yyyy}_v2.nc

with ${yyyy} any year between 1961 and 2020.

4.1.1 Contact persons:

philippe.ciais@lsce.ipsl.fr;

frederic.chevallier@lsce.ipsl.fr

5 Regional biogenic prior emission datasets for 2018 and 2021 (2017-2021)

5.1 Model

For the European domain, biogenic fluxes at ~1-km resolution for GPP and respiration have been prepared based on the diagnostic light-use-efficiency model VPRM (Vegetation Photosynthesis Respiration Model, Mahadevan et al., 2008). This simple model is driven by indices derived from satellite measurements, namely the enhanced vegetation index (EVI) and the land surface water index (LSWI) as well meteorological data. The remotely sensed indices EVI and LSWI are calculated based on 8-day reflectances measured by MODIS (product MOD09A1, version 6), which are measured at spatial resolutions between 500 m and 1 km. A loess filter is applied to the signals at the pixel scale. Hourly meteorological (2-m temperature and shortwave radiation at the surface) are taken from the ECMWF ERA5 reanalysis data at 0.25° resolution.

The model considers the fractional coverage of seven different land cover classes, currently defined by the landcover map SYNMAP (Jung et al., 2006). For each of the landcover types two parameters are fit to match measurements from local flux tower sites from a different year. In this case, the parameters were fit based on a selection of representative European sites for each landcover type using data for the year 2007, retrieved from www.europe-fluxdata.eu. For more information about which sites were used and the parameter values we refer to Gerbig (2021).

5.2 Spatial coverage and resolution

The fluxes were computed over the larger domain that is used for the TNO anthropogenic fluxes, but at the spatial resolution of the higher-resolution TNO fluxes. Specifically, the fluxes cover a spatial domain of 30° latitude to 72° latitude, and 30° W to 60°E longitude.

The spatial resolution of the domain is 1/120° in the latitudinal direction, and 1/60° in the longitudinal direction. Over Central Europe, this approximates 1-km spatial resolution. The latitude and longitude coordinates given in the data files represent the lower left corner of the grid boxes. Rather than store the pixel area in each file, the area of the pixels (for all regions) are provided in the file CoCO2_VPRM_areas.nc.

5.3 Regional blocks

Because the targeted spatial resolution is very high, storing the whole domain within one file results in rather large files. Instead, the domain is split into six tiles, each covering a domain of 30° longitude and 21° latitude, with 1800 pixels in the west-east direction and 2520 pixels in the south-north direction. The regions are plotted in Figure 13, and the coordinates of the lower-left and upper-right corners are given in Table 5.

Table 5 Overview of the extent of each sub-domain.

Region	Lower left corner (lat, lon)	Upper right corner (lat, lon)
Reg1	51° N, 30° W	72° N, 0°
Reg2	51° N, 0°	72° N, 30° E
Reg3	51° N, 30° E	72° N, 60° E
Reg4	30° N, 30° W	51°N, 0°
Reg5	30°N, 0°	51°N, 30° E
Reg6	30°N, 30° E	51°N, 60° E

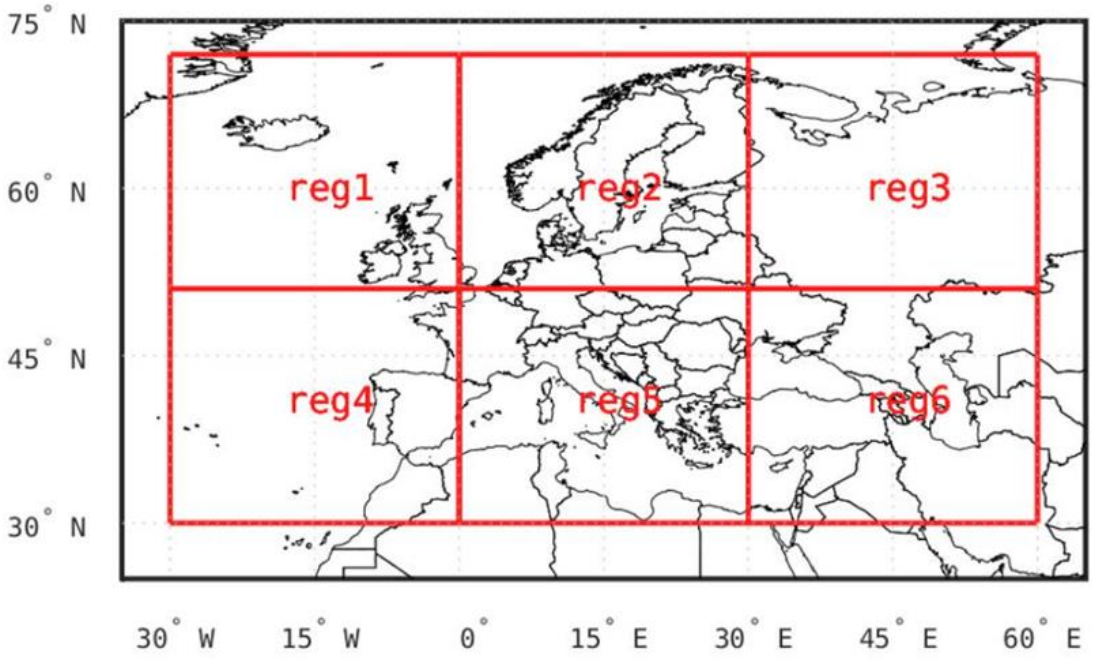

Figure 13 The spatial extent of each of the six sub-domains on which the VPRM fluxes were calculated.

5.4 Temporal resolution

The temporal resolution of the fluxes is hourly, following that of the ERA5 driving meteorology. Important: the time stamp in the matches that of the meteorological data, and the downwelling shortwave radiation at the surface is an accumulated parameter. Thus, the value at e.g. 12:00 represents the mean radiation between 11:00 and 12:00. As such, the recommendation is to use this flux in the transport model for the time between 11:00 and 12:00. Thus, the time stamp in the model can be seen as the end of the valid period. If modelling the full year, this means that there is no data point for 23:00 on December 31st, but here the previous hour could simply be repeated.

5.5 Data Access

The fluxes have been extended for the period from 2017 and 2021, and can be accessed under the following links:

2017: https://swiftbrowser.dkrz.de/public/dkrz_713c5812-40a6-4d9c-a938-50cfce20c44f/CoCO2_VPRM_fluxes_2017/

2018: https://swiftbrowser.dkrz.de/public/dkrz_713c5812-40a6-4d9c-a938-50cfce20c44f/CoCO2_VPRM_fluxes_2018/

2019:https://swiftbrowser.dkrz.de/public/dkrz_713c5812-40a6-4d9c-a938-50cfce20c44f/CoCO2_VPRM_fluxes_2019/

2020: https://swiftbrowser.dkrz.de/public/dkrz_713c5812-40a6-4d9c-a938-50cfce20c44f/CoCO2_VPRM_fluxes_2020/

2021: https://swiftbrowser.dkrz.de/public/dkrz_713c5812-40a6-4d9c-a938-50cfce20c44f/CoCO2_VPRM_fluxes_2021/

More details on how to access the data can be found here Task 4.4 Confluence page (readme)

5.5.1 Contact person:

Julia Marshall, DLR – julia.marshall@dlr.de

6 Global biogenic prior emission datasets for 2021

Biogenic carbon flux estimates based on integrating in-situ observations and satellite data using machine-learning methods are provided from the Fluxcom approach (Jung et al. 2020, www.fluxcom.org). In this, statistical relationships between in-situ observations of carbon fluxes and environmental conditions are learned and transferred to global gridded estimates using satellite observations and meteorological data of the same predictors. Data simulated with the newly implemented modelling framework Fluxcom2.0 following this methodological approach (publication in preparation) will be provided.

6.1 Details of data processing:

We combine sets of eddy-covariance data collections, namely the Fluxnet2015 (Pastorello et al. 2020), ICOS Drought 2018 (ICOS Drought 2018) and ICOS Warm Winter 2020 (ICOS WarmWinter2020) initiatives. From these we work with hourly net and gross carbon fluxes, with the latter using nighttime partitioning (Reichstein et al. 2005) only.

The set-up foresees predictor variables that inform the machine learning algorithm on a range of time scales:

Annual:

- vegetation type (in a fuzzy translation of plant functional types into classes of trees, shrubs, grasses, crops, wetland, C4_photosynthesis, needleleaf, broadleaf, deciduous, evergreen for generalizability across land cover classifications using different classes)

Daily:

- MODIS derived Enhanced vegetation index, near-infrared reflectance of vegetation
- MODIS TERRA land surface temperature

Hourly:

- potential radiation
- derivative of potential radiation
- surface short-wave radiation
- air temperature
- vapour pressure deficit

Eddy-covariance station measurements undergo quality filtering according to the quality information in the flux data releases, as well as a complementary and automated inspection approach that flags data samples of one variable if their relationship with samples of other related variables is inconsistent (details about this new quality assessment of eddy-covariance data sets are in preparation for submission as a manuscript, Jung et al. in prep). About 13 million good quality hourly samples from 249 sites constitute the training basis for NEE (similar for GPP).

Site-level remotely sensed data from MODIS instruments are extracted and processed after Walther & Besnard et al. (2022). Global reflectance data use the MCD43C4 product (Schaaf et al. 2015) and global LST the MOD11C1 (Wan et al. 2015) product. They undergo a preprocessing that is consistent with the site-level data.

Global atmospheric information stems from the ERA5 meteorological fields (Hersbach et al. 2020) except for the potential shortwave radiation which is computed according to Pastorello et al (2019).

As a machine learning method we opted for the boosted regression tree ensemble (in the XGBoost implementation, Chen and Guestrin, 2016; Elith et al., 2008).

6.2 Results for Net Ecosystem Exchange

The following focuses on the results for NEE, though GPP estimates are also provided to the project.

Evaluation of the NEE estimates of a ten-fold leave-sites-out cross-validation across a range of temporal scales shows reliable prediction accuracy in terms of the Nash-Sutcliffe modelling efficiency (NSE) for the hourly time step (NSE=0.761), as well as regular patterns such as the mean seasonal (NSE=0.7) and diurnal cycles (NSE=0.860). With NSE of 0.315 and 0.413, respectively, deviations from the average annual cycle and spatial patterns are moderately reliably represented at site level. Interannual NEE variations have no skill (NSE=0.074) at site level.

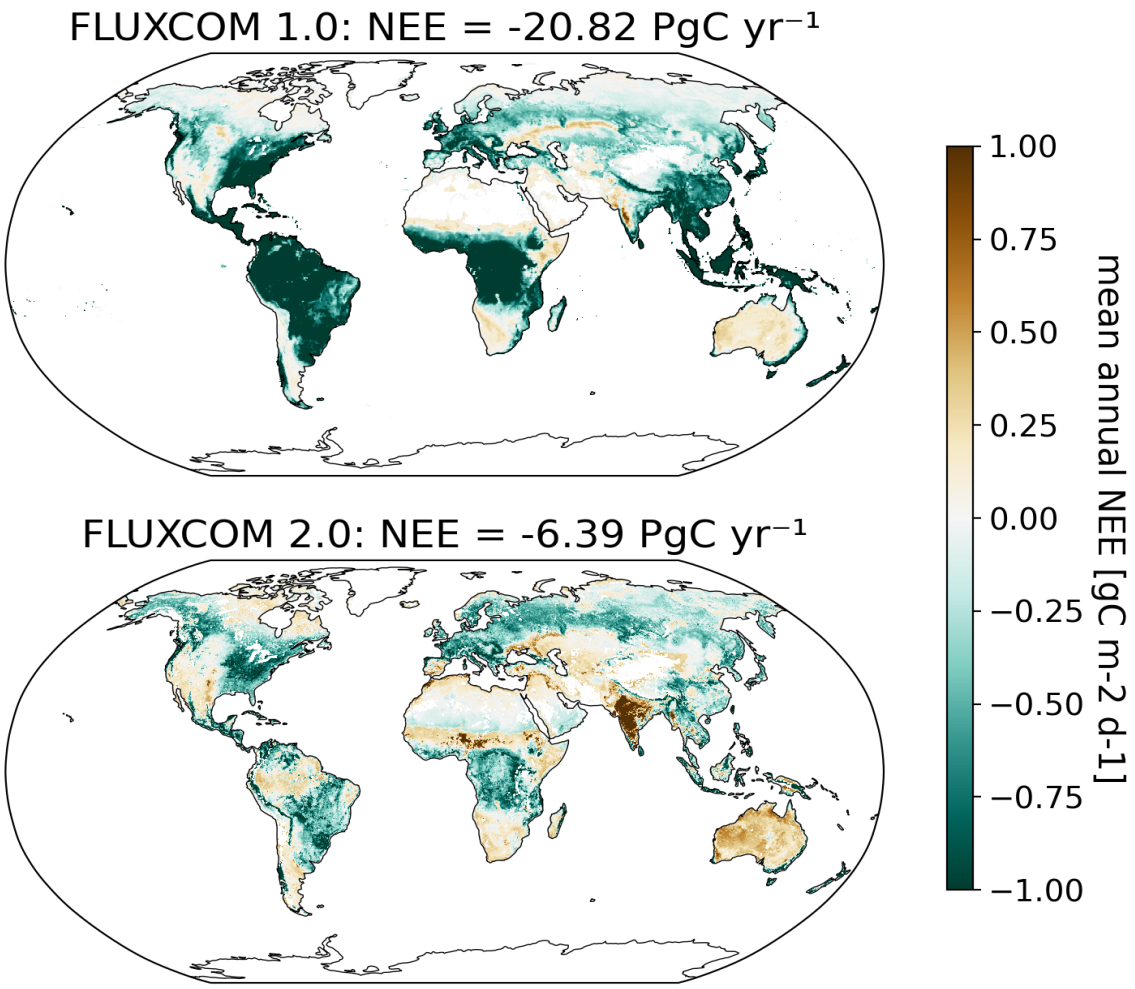

Figure 14: Annual net biogenic carbon uptake averaged over 2018-2021 as compared from Fluxcom1.0 (Fluxcom-RS+meteo ensemble estimates, according to Jung et al. 2020) and the set-up in the new modelling framework Fluxcom 2.0.

Global annual NEE estimates from this set-up in the new modelling framework are drastically lower than previous data-driven estimates from Fluxcom (Figure 14, Fluxcom1.0 in this case refers to the ensemble estimate of the Fluxcom-RS+Meteo set-up according to Jung et al. (2020), and NOT to the data version submitted to the project for the year 2018). In particular, the previously very strong sinks in the tropical evergreen forests result much less strong in the updated estimates, with the central Amazon region even reversing to a net source. Except for the central Amazon, Fluxcom1.0 and Fluxcom2.0 qualitatively agree on whether large scale

regions act as carbon sinks or sources on average, but Fluxcom2.0 consistently predicts less strong sinks (e.g. central European and eastern North American temperate ecosystems) and stronger sources (especially in India, large parts of Australia, and the Sahel). The updated global biogenic sink amounts to -6.39PgC, compared to -20.82PgC per year in Fluxcom1.

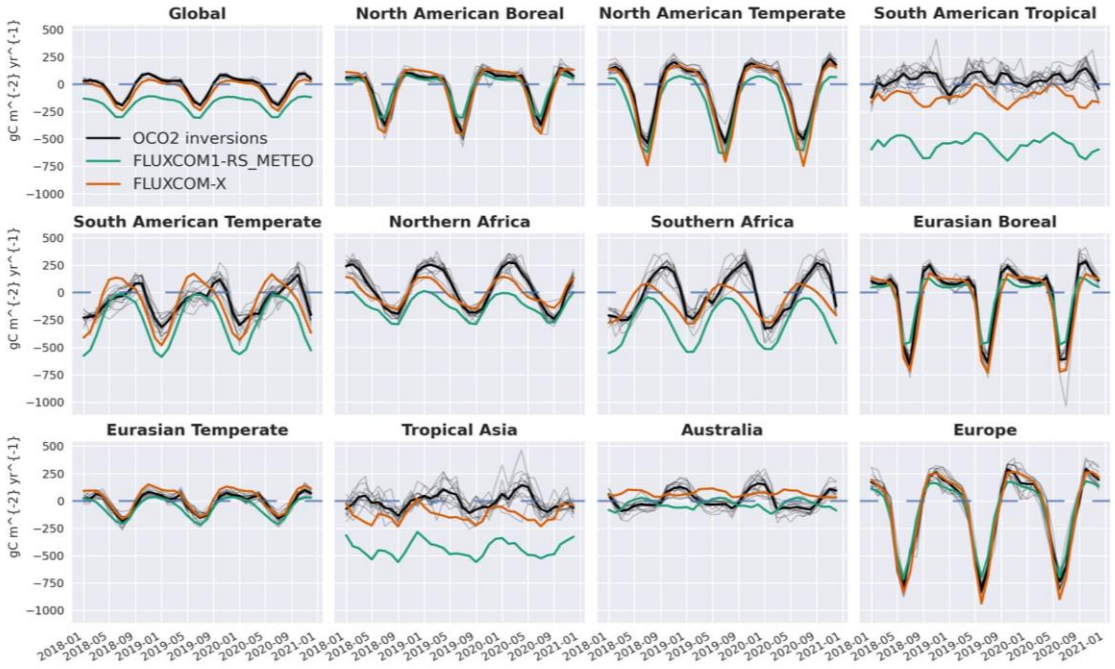

Figure 15: Net monthly carbon uptake estimates averaged over large scale regions, comparing Fluxcom1-RS+meteo ensemble, the current Fluxcom2.0 and OCO-2 MIP inversions. The 'OCO2-inversions' are an ensemble of atmospheric inversions that combine atmospheric CO2 concentrations from both in-situ observations and satellite-derived atmospheric mixing ratios from OCO2, data shown here are from the LNLGISS experiment using ACOS XCO2 v10, data courtesy Brendan Byrne and OCO-MIP team, Byrne et al. (2022).

Quantitatively the current average sink magnitude agrees significantly better with atmospheric inversion estimates (Figure 15). Over large scale regions of the Earth the bias between top-down and bottom-up estimates is clearly reduced. Qualitatively the temporal trajectories are very similar between Fluxcom1.0 and Fluxcom2.0, but markedly dissimilar from the atmospheric inversions in all but European and North American regions. Note, that in this comparison, emissions originating from fires are not yet accounted for.

6.3 Details and access of global biogenic flux data

Global hourly estimates of NEE and GPP span the period 2018-2021 (will be extended back to 2001) at a spatial resolution of 0.05deg. These data can be access via a password protected MinIO server, an example of how to access can be found in the example Jupyter Notebook (https://nextcloud.bgc-jena.mpg.de/s/8L9DHoRRxrS9cb6, password required, please use the contact details below to obtain the password).

6.3.1 Contact persons:

Martin Jung mjung@bgc-jena.mpg.de;

Jacob A. Nelson jnelson@bgc-jena.mpg.de;

Sophia Walther swalth@bgc-jena.mpg.de

7 Global ocean flux datasets for 2021

In the framework of the WP2.2, Mercator Ocean has proposed an evolution of the air-sea CO2 flux stream as inputs to the ECMWF-IFS: from the use of the low resolution and daily JENA-MLS air-sea CO2 product in the current configuration (*cf.* Figure 16), to the use of a high-resolution and daily data-assimilated air-sea CO2 flux product provided by the Copernicus Marine Monitoring Service (hereafter CMEMS) (*cf.* Figure 17).

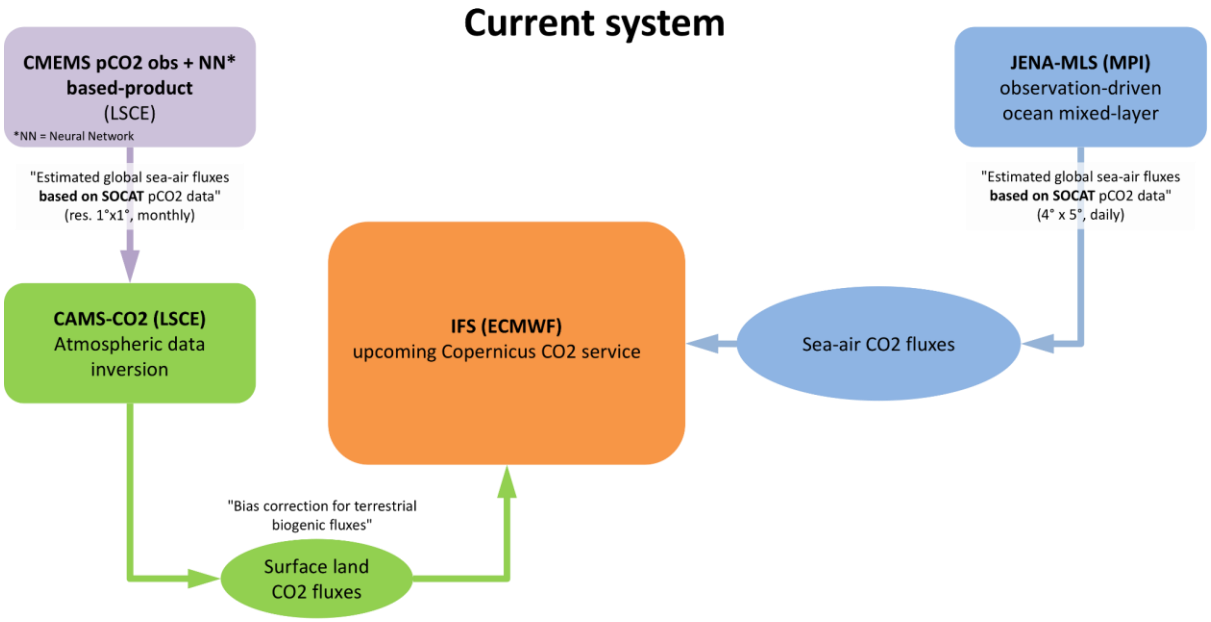

Figure 16: Schematic of the CO2 flux streams in the current IFS

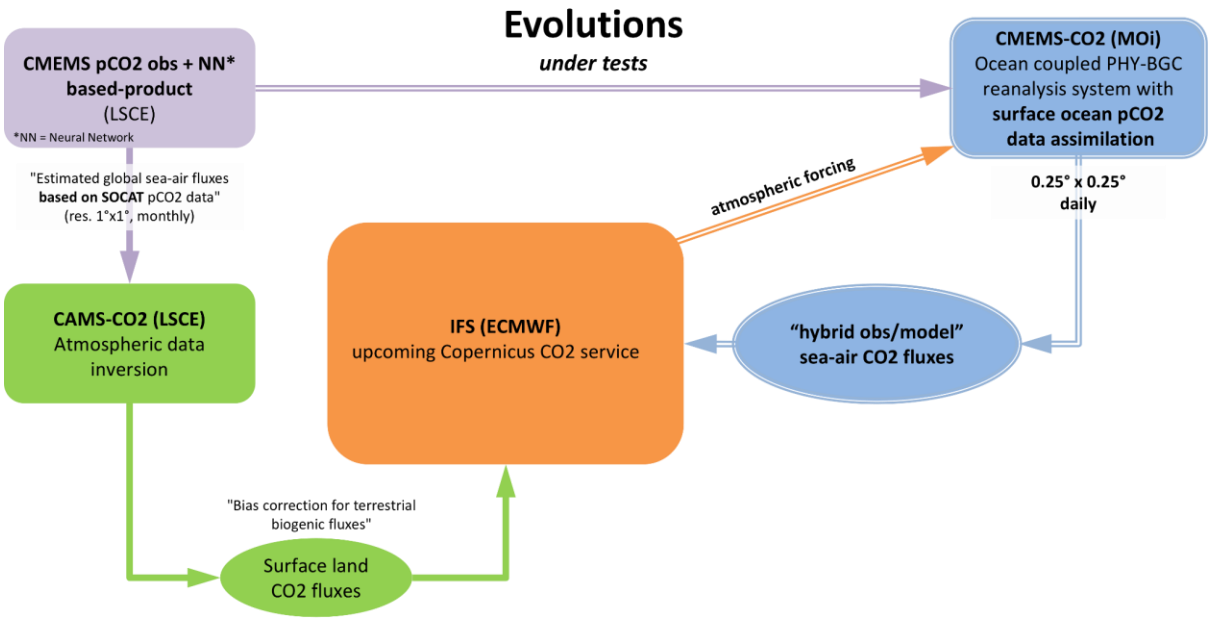

Figure 17: Schematic of the proposed evolution of sea-air CO2 flux stream in the future IFS

This evolution relies on the CMEMS Global modelling and data-assimilating biogeochemical system, operated at Mercator Ocean. In this system, we implemented the assimilation of surface pCO2 maps - provided in the CMEMS MOB-TAC product developed by LSCE - that allows to calculate a large-scale correction of the modelled air-sea CO2 flux. In this first prototype, this correction is applied “offline” i.e. the information brought by the observations are not directly injected into the “dynamics” of the model’s carbonates component. Therefore, this methodology (1) adjusts - by construction - the large-scale structures of the modelled air-sea CO2 fluxes towards the large-scale structures from the CMEMS MOB-TAC observation-based product (taking into account the error budget from the observation product) and (2) preserves the meso-scale dynamical structures in the air-sea CO2 flux computed by the BGC model. The resulting “hybrid” observations/model product is hence provided on a 1/4° ORCA-grid, with a daily frequency.

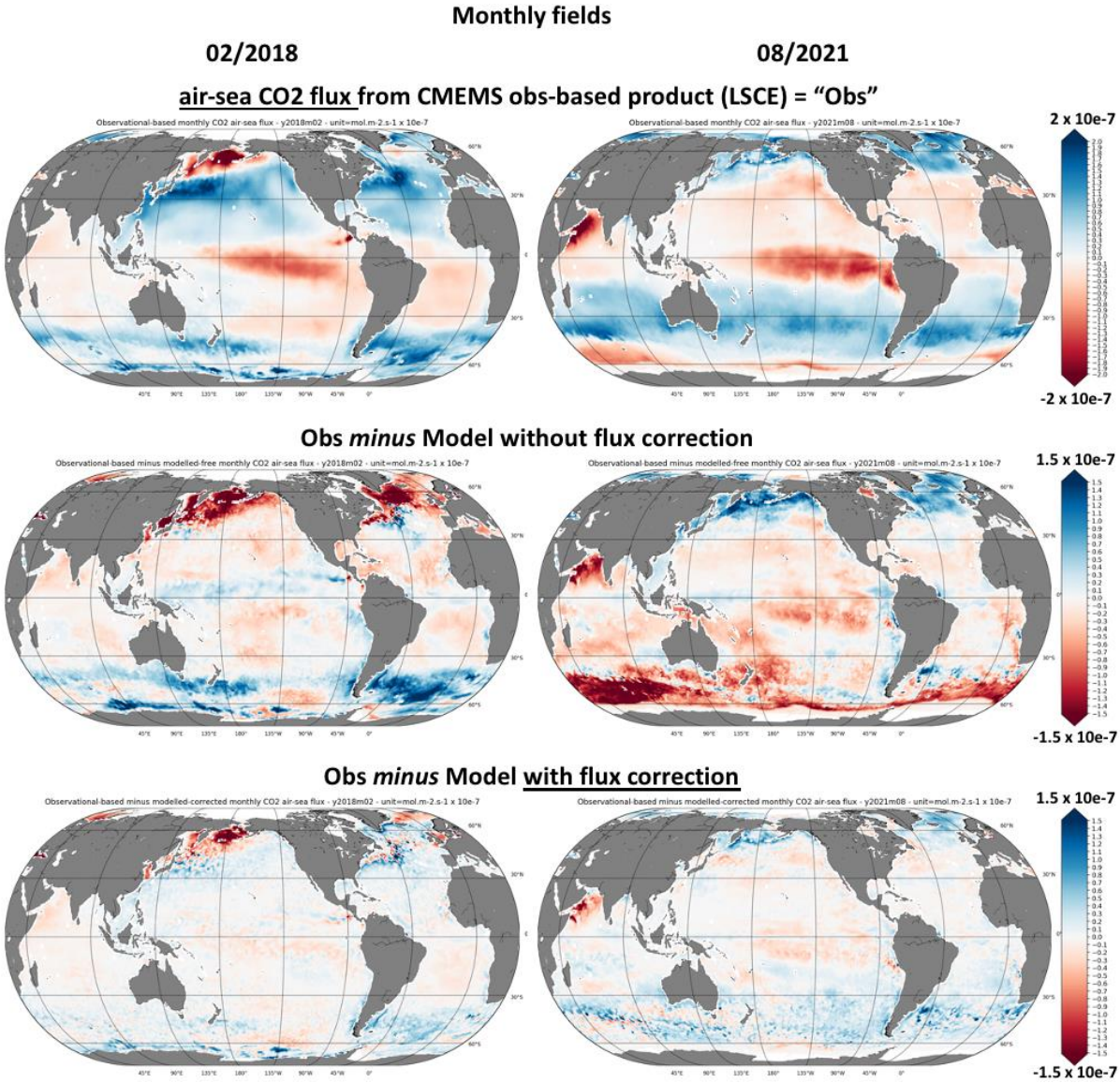

Figure 18: illustration of the impact of the air-sea CO2 flux correction: [top row] reference observation of air-sea CO2 flux from the Copernicus Marine Service MOB-TAC product, and difference between [mid-row] the reference observation and the uncorrected air-sea CO2 flux, and [bottom row] the reference observation and corrected air-sea CO2 flux.

Figure 18 proposes an illustration of the impact of the air-sea CO2 flux correction; it compares the full-resolution air-sea CO2 flux from the BGC model, with or without the flux correction, to the air-sea CO2 flux from the CMEMS MOB-TAC observation product (projected on the model 1/4° grid). The large-scale bias between the model and the observation are shown to be significantly reduced in the flux-corrected simulation (as expected, and by construction). Some very localized discrepancies remain (cf. in Bering Sea), and might be due to some differences - between the model and the observation-based product - in the parameterisations of the air-sea CO2 flux computation (e.g. different wind forcings). The short-scale structures visible in the bias between the observation and the flux-corrected model, are the signature of the meso-scale activity, brought by the dynamically-forced BGC model, into this “hybrid” product.

In addition, Figure 19 confirms the methodology efficiency, by intercomparing the global averaged spCO2 and global budget of air-sea CO2 flux, from the “hybrid” model/obs product (in pink), to various observation-based products (e.g. Landschutzer product). In the common period, the “hybrid” model/obs product compares well with the observation-based products, when it comes to both trends and amplitudes.

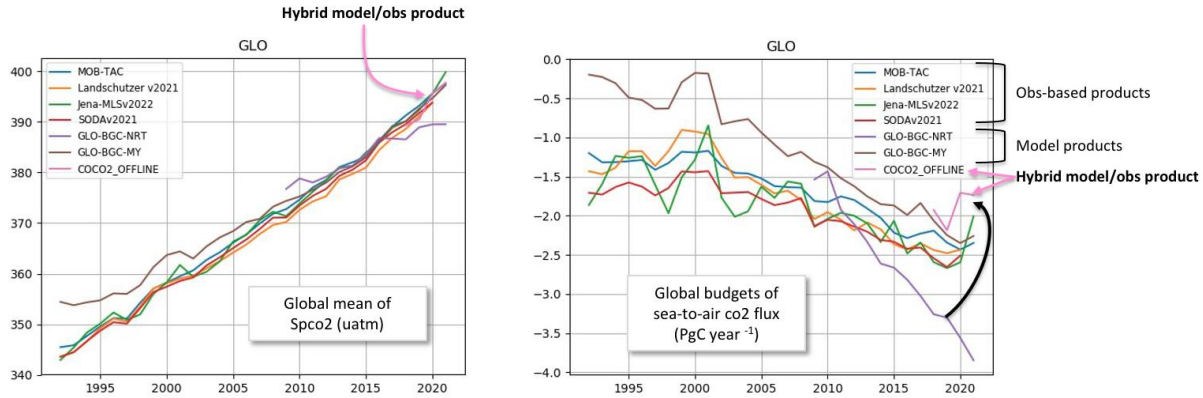

Figure 19: [left] global mean of spCO2 and [right] associated global budgets of sea-air CO2 flux, for various observation-based and model-based products.

A whole set of air-sea CO2 flux, covering 2018 and 2021 at 1/4° resolution and daily frequency, has been provided to Anna Agusti-Panareda. First assessments of the impact of these fluxes onto IFS atmospheric pCO2 outputs are ongoing and seem encouraging.

7.1 Data availability

The air-sea CO2 flux data are available on various grids from the Mercator ocean ftp site (ftp.mercator-ocean.fr). For access details please contact the person given in section 7.1.1.

- the daily corrected fluxes, covering **20/12/2017 to 15/01/2019**, on our **ORCA grid**:
  => ***concat_BIOMER_corrected_cflx_20171220_20190115.nc***
- Same, but interpolated on a **regular grid:**
  => ***concat_BIOMER_corrected_cflx_20171220_20190115_REGULAR_GRID.nc***

- the daily corrected fluxes, covering **20/12/2020 to 28/01/2021**, on our **ORCA grid**:
  => ***concat_BIOMER_corrected_cflx_20201220_20211228.nc***
- Same, but interpolated on a **regular grid:**
  => ***concat_BIOMER_corrected_cflx_20201220_20211228_REGULAR_GRID.nc***

7.1.1 Contact persons:

Coralie Perruche cperruche@mercator-ocean.fr,

Julien Lamouroux jlamouroux@mercator-ocean.fr

8 LULUCF datasets for 2018-2020

For the global net flux of CO_2 from land use, land-use change, and forestry (LULUCF), JRC compiled a dataset that builds on national greenhouse gas inventories (NGHGIs) communicated via a range of country reports to the UNFCCC. Specifically, for Annex I countries, data are sourced from annual GHG inventories. For non-Annex I countries, data are based on the most recent and complete information from different sources, including national communications, biennial update reports, submissions to the REDD+ (reducing emissions from deforestation and forest degradation) framework, and nationally determined contributions. The data are disaggregated into fluxes from forest land, deforestation, organic soils, and other sources (including non-forest land uses). To ensure completeness of time series, for developing countries data are gap filled with standard procedures.

Results indicate a mean net global sink of 1.6 GtCO2 yr-1 over the period 2000–2020, largely determined by a large sink on forest land, partially compensated by sources from deforestation.

Overall, while the quality and quantity of the LULUCF data submitted by countries to the UNFCCC significantly improved in recent years, important gaps still remain. Most developing countries still do not explicitly separate managed vs. unmanaged forest land, a few report implausibly high forest sinks, and several report incomplete estimates. With these limits in mind, the database presented here represents the most up-to-date and complete compilation of LULUCF data based on country submissions to UNFCCC.

8.1 Documentation

Grassi G., et al. (2022) Carbon fluxes from land 2000–2020: bringing clarity on countries' reporting. Earth Syst. Sci. Data, 14, 4643–4666, 2022

8.2 Data access

Data from this study are openly available via the Zenodo portal (Grassi et al., 2022), at https://doi.org/10.5281/zenodo.7190601.

8.2.1 Contact person:

Giacomo.Grassi@ec.europa.eu

9 Emission height profiles by source sector

Individual emission height profiles for specific industrial facilities (i.e., top emitters) could be developed and provided as a next step. Prior to that, interaction with modellers is needed to understand their requirements and identify how the representation of point sources in the proposed case studies can be improved. The following subsections describe the sector-dependent emission height profiles proposed as a first step for the vertical distribution of the regional and global anthropogenic prior emission datasets, respectively.

9.1 Regional emission height profiles

Table 6summarises the TNO default emission height profiles proposed by GNFR sector. The information is derived from Table 3 in Bieser et al. (2011). The lowest layer over 0-92 m is split into a surface part for 0-20 m and remainder, to better facilitate simulation models that usually have a first layer of this thickness. Surface emissions are then 100% assigned to this 0-20 m layer. The table shows height distributions as fractions (0-1) for the different layers. The header shows the top of the layer in m. Future tasks will include a comparison of the vertical profile proposed for sector GNFR_A (public energy) with the one derived from the plume rise calculations performed under Task 2.4.

Table 6 Sector-dependent emission height profiles proposed for regional anthropogenic prior emission datasets

GNFR Category	0-20m	20-92m	92-184m	184-324m	324-522m	522-781m	781-1106m
A	0	0	0.0025	0.51	0.453	0.0325	0.002
B	0.06	0.16	0.75	0.03	0	0	0
C	1	0	0	0	0	0	0
D	0.02	0.08	0.6	0.3	0	0	0
E	1	0	0	0	0	0	0
F1	1	0	0	0	0	0	0
F2	1	0	0	0	0	0	0
F3	1	0	0	0	0	0	0
F4	1	0	0	0	0	0	0
G	0.2	0.8	0	0	0	0	0
H	0.25	0.25	0.1	0.1	0.1	0.1	0.1
I	1	0	0	0	0	0	0
J	0	0.41	0.57	0.02	0	0	0
K	1	0	0	0	0	0	0
L	1	0	0	0	0	0	0

9.1.1 contact persons

hugo.deniervandergon@tno.nl

jeroen.kuenen@tno.nl

9.2 Global emission height profiles

Table 7 summarises the simplified sector-dependent emission height profiles proposed as a first step for the vertical distribution of global anthropogenic emissions. For the public energy sector (ene), CO2 emission-weighted plume bottom and top values were derived from the global plume rise calculations performed in CoCO2 Task 2.4 combining the CoCO2 global point source database with meteorological information. The final values correspond to the first quartile (plume bottom) and third quartile (plume top) of the collection of simulated plant-level annual plume bottom and top values. For the other sectors, the information is derived from the height profiles proposed for the regional scale (previous section). For the sectors not included in the table all emissions should be injected at the surface level.

Table 7 Sector-dependent emission height profiles proposed for global anthropogenic prior emission datasets

Sector	Description	Injection height [m]
ene	Power generation	240 - 745
ind	Industrial process	20 - 300
shp	Shipping	30 - 100
swd (*)	Solid waste and waste water	20 - 100
(*) only applicable to emissions mainly related to incineration plants and open burning of waste (i.e. NOx, CO, NMVOC, SO2, PM10, PM2.5, CO2). CH4 and NH3 are mainly diffuse emissions from solid waste disposal sites and water waste treatment plants and should be injected at the surface level		

9.2.1 contact person:

marc.guevara@bsc.es

10 References

Bieser, J., Aulinger, A., Matthias, V., Quante, M., Denier van der Gon, H.A.C.: Vertical emission profiles for Europe based on plume rise calculations, Environmental Pollution, Volume 159, Issue 10, 2011, Pages 2935-2946, doi:10.1016/j.envpol.2011.04.030.

Byrne et al. 2022, 'National CO_2 budgets (2015–2020) inferred from atmospheric CO_2 observations in support of the Global Stocktake', https://essd.copernicus.org/preprints/essd-2022-213/

Chen et al. 2016, 'XGBoost: A Scalable Tree Boosting System', http://dx.doi.org/10.1145/2939672.2939785

Ciais, P., Bastos, A., Chevallier, F., Lauerwald, R., Poulter, B., Canadell, J. G., Hugelius, G., Jackson, R. B., Jain, A., Jones, M., Kondo, M., Luijkx, I. T., Patra, P. K., Peters, W., Pongratz, J., Petrescu, A. M. R., Piao, S., Qiu, C., Von Randow, C., Regnier, P., Saunois, M., Scholes, R., Shvidenko, A., Tian, H., Yang, H., Wang, X., and Zheng, B.: Definitions and methods to estimate regional land carbon fluxes for the second phase of the REgional Carbon Cycle Assessment and Processes Project (RECCAP-2), Geosci. Model Dev., 15, 1289–1316, https://doi.org/10.5194/gmd-15-1289-2022, 2022.

Ciais, P., P. Bousquet, A. Freibauer, T. Naegler. Horizontal displacement of carbon associated with agriculture and its impacts on atmospheric CO 2. Global Biogeochemical Cycles, American Geophysical Union, 2007, 21 (2), pp.GB2014. ff10.1029/2006gb002741

CMT, 2021, Global Coal Mine Tracker, online database. URL: https://globalenergymonitor.org/projects/global-coal-mine-tracker/

Deng, Z., Ciais, P., Tzompa-Sosa, Z. A., Saunois, M., Qiu, C., Tan, C., Sun, T., Ke, P., Cui, Y., Tanaka, K., Lin, X., Thompson, R. L., Tian, H., Yao, Y., Huang, Y., Lauerwald, R., Jain, A. K., Xu, X., Bastos, A., Sitch, S., Palmer, P. I., Lauvaux, T., d'Aspremont, A., Giron, C., Benoit, A., Poulter, B., Chang, J., Petrescu, A. M. R., Davis, S. J., Liu, Z., Grassi, G., Albergel, C., and Chevallier, F.: Comparing national greenhouse gas budgets reported in UNFCCC inventories against atmospheric inversions, Earth Syst. Sci. Data, accepted, 2022.

Elith et al. 2008, 'A working guide to boosted regression trees', https://besjournals.onlinelibrary.wiley.com/doi/abs/10.1111/j.1365-2656.2008.01390.x

Gerbig, C. (2021). Parameters for the Vegetation Photosynthesis and Respiration Model VPRM (Version 1.0). ICOS-ERIC - Carbon Portal. https://doi.org/10.18160/R9X0-BW7T

GIE, 2018, Storage Database. Gas Infrastructure Europe. URL: https://www.gie.eu/index.php/gie-publications/databases/storage-database

Grassi, G., Stehfest, E., Rogelj, J. *et al.* Critical adjustment of land mitigation pathways for assessing countries' climate progress. *Nat. Clim. Chang.* **11,** 425–434 (2021). https://doi.org/10.1038/s41558-021-01033-6

Guevara, M., Petetin, H., Jorba, O., Denier van der Gon, H., Kuenen, J., Super, I., Jalkanen, J.-P., Majamäki, E., Johansson, L., Peuch, V.-H., and Pérez García-Pando, C.: European primary emissions of criteria pollutants and greenhouse gases in 2020 modulated by the COVID-19 pandemic disruptions, Earth Syst. Sci. Data, 14, 2521–2552, https://doi.org/10.5194/essd-14-2521-2022, 2022.

Hersbach et al. 2020, 'The ERA5 global reanalysis', https://doi.org/10.1002/qj.3803

ICOS Drought 2018 Dataset, 'Drought 2018 Team and ICOS Ecosystem Thematic Centre: Drought-2018 ecosystem eddy covariance flux product for 52 stations in FLUXNET-Archive format', https://doi.org/10.18160/YVR0-4898

ICOS Warm Winter 2020 Dataset, 'Warm Winter 2020 ecosystem eddy covariance flux product for 73 stations in FLUXNET-Archive format—release 2022-1', https://doi.org/10.18160/2G60-ZHAK

Jalkanen, J.-P.P., brink, A., Kalli, J., Pettersson, H., Kukkonen, J., Stipa, T., Kuukkonen, J., and T. Stipa, Kukkonen, J., Stipa, T., 2009. A modelling system for the exhaust emissions of marine traffic and its application in the Baltic Sea area. Atmos. Chem. Phys. 9, 9209–9223. https://doi.org/10.5194/acp-9-9209-2009

Jalkanen J.-P., E. Majamäki, Improve the ship emissions applying the FMI approach to emission modelling, Deliverable report CAMS81_2020SC1_ D81.2.3.1_Improved ship emissions for 2014-2020, CAMS, 2021

Jung, M., Henkel, K., Herold, M., and Churkina, G.: Exploiting synergies of global land cover products for carbon cycle modeling, Remote Sens. Environ., 101, 534–553, 2006.

Jung et al. 2020, 'Scaling carbon fluxes from eddy covariance sites to the globe: synthesis and evaluation of the FLUXCOM approach', https://bg.copernicus.org/articles/17/1343/2020/

Liu, Z., Ciais, P., Deng, Z. et al. Carbon Monitor, a near-real-time daily dataset of global CO2 emission from fossil fuel and cement production. Sci Data 7, 392 (2020). https://doi.org/10.1038/s41597-020-00708-7

Mahadevan, P., Wofsy, S. C., Matross, D. M., Xiao, X., Dunn, A. L., Lin, J. C., Gerbig, C., Munger, J. W., Chow, V. Y., and Gottlieb, E. W. (2008), A satellite-based biosphere parameterization for net ecosystem CO2 exchange: Vegetation Photosynthesis and Respiration Model (VPRM), Global Biogeochem. Cycles, 22, GB2005, doi:10.1029/2006GB002735.

Pastorello et al. 2019, 'ONEFlux: Open Network-Enabled Flux processing pipeline', https://github.com/AmeriFlux/ONEFlux/

Pastorello et al. 2020, 'The FLUXNET2015 dataset and the ONEFlux processing pipeline for eddy covariance data', https://doi.org/10.1038/s41597-020-0534-3

Reichstein et al. 2005, 'On the separation of net ecosystem exchange into assimilation and ecosystem respiration: review and improved algorithm', https://doi.org/10.1111/j.1365-2486.2005.001002.x

Schaaf et al. 2015, 'MCD43C4 MODIS/Terra+Aqua BRDF/Albedo Nadir BRDF-Adjusted Ref Daily L3 Global 0.05Deg CMG V006 [Data set]. NASA EOSDIS Land Processes DAAC.' https://doi.org/10.5067/MODIS/MCD43C4.006

Walther & Besnard et al. 2022, 'Technical note: A view from space on global flux towers by MODIS and Landsat: the FluxnetEO data set', https://bg.copernicus.org/articles/19/2805/2022/

Wan et al. 2015, 'MOD11C1 MODIS/Terra Land Surface Temperature/Emissivity Daily L3 Global 0.05Deg CMG V006 [Data set]. NASA EOSDIS Land Processes DAAC.', https://doi.org/10.5067/MODIS/MOD11C1.006

Document History

Version	Author(s)	Date	Changes
	Name (Organisation)	dd/mm/yyyy	
V1.0	Hugo Denier van der Gon (TNO)	18/11/2022	
V1.1	Hugo Denier van der Gon (TNO) and chapter responsible teams	21/12/2022	Revised and/or completed chapters
V1.2	Hugo Denier van der Gon (TNO)	01/02/2023	Revision and clarifications as requested by the internal reviewers

Internal Review History

Internal Reviewers	Date	Comments
Anusha.Sunkisala (DWD)	06/01/2023	By email on date indicated
Dario Papale (CMCC)	29/12/2022	By email on date indicated

Estimated Effort Contribution per Partner

Partner	Effort
TNO	6
CNRS-LA	*12*
DLR	1
MPG	2.5
BSC	1
MOi	15
CEA	2
JRC	*0.5*
Total	40